Int J Fract (2015) 196:33–57
DOI 10.1007/s10704-015-0038-x

SPECIAL INVITED ARTICLE CELEBRATING IJF AT 50

Recent developments in dynamic fracture: some perspectives

Jay Fineberg · Eran Bouchbinder

Received: 24 April 2015 / Accepted: 1 August 2015 / Published online: 13 August 2015

Abstract We briefly review a number of important recent experimental and theoretical developments in the field of dynamic fracture. Topics include experimental validation of the equations of motion for straight tensile cracks (in both infinite media and strip geometries), validation of a new theoretical description of the near-tip fields of dynamic cracks incorporating weak elastic nonlinearities, a new understanding of dynamic instabilities of tensile cracks in both 2D and 3D, crack front dynamics, and the relation between frictional motion and dynamic shear cracks. Related future research directions are briefly discussed.

Keywords Dynamic fracture · Singularities and instabilities · Friction

1 Introduction

The goal of this paper is to offer some perspectives on a number of significant developments in the field of dynamic fracture that have taken place over the past decade or so. The subjects that we chose to describe are topics that we have worked on, so this paper is, by definition, quite subjective. We believe that in these chosen areas there has been significant progress—and each is interesting in its own right. We will make no attempt to present any of these subjects in depth. The idea is to present a schematic, non-technical, overview of the main discoveries and fundamental insights that have evolved from recent research in each of these different areas. Many of these topics have been driven forward by new experiments that have utilized a variety of new techniques to obtain measurements that had not previously been possible. In these cases, comparison of these experiments to the existing theoretical predictions revealed previously unappreciated gaps in our understanding. These, in turn, provided incentives to expand the theoretical framework to encompass these observations. Some, but not all, of the topics addressed in this perspective piece were systematically reviewed in two relatively recent review papers (Bouchbinder et al. 2010a, 2014). Our goal here, as explained above, is different.

The structure of this paper is as follows. In Sect. 2 we consider the equation of motion for dynamic tensile (mode I) cracks that has been predicted in the framework of Linear Elastic Fracture Mechanics (LEFM). We will describe recent experiments that have quantitatively shown that the ideas of energy balance that had been the cornerstone of dynamic fracture mechanics indeed provide an excellent quantitative description of crack dynamics as long as rapid fracture is mediated by single "simple" cracks; i.e. cracks that prop-

J. Fineberg (✉)
Racah Institute of Physics, Hebrew University of Jerusalem, Jerusalem 91904, Israel
e-mail: jay@mail.huji.ac.il

E. Bouchbinder
Chemical Physics Department, Weizmann Institute of Science, Rehovot 7610001, Israel
e-mail: eran.bouchbinder@weizmann.ac.il

agate along prescribed paths and have not undergone dynamic instabilities.

Section 3 considers the form of the singular fields surrounding the tips of these "simple" cracks. We first discuss a few rather peculiar features of the $\sqrt{r}$ singular fields predicted by LEFM. We then show that experiments which utilize soft materials to "slow down" crack dynamics, making them accessible to direct measurements, revealed that the fields in the vicinity of dynamic crack tips may significantly deviate from the LEFM predictions. These fields were explained by theoretically incorporating the leading nonlinear elastic behavior of the medium that becomes important at the high strains that invalidate LEFM as the tip is approached. This theory also predicts the existence of a new intrinsic length scale emerging from the competition between linear and nonlinear elastic constitutive behaviors. Thus, while energy balance predicts the overall dynamics of simple cracks, the structure of the elastic fields driving fracture is modified by elastic nonlinearities near the crack's tip, where linear elasticity starts to break down.

In Sect. 4 we go on to consider tensile cracks that are no longer simple. This happens when simple cracks become unstable to different instabilities. We briefly mention the micro-branching instability, where frustrated microscopic branches are spawned at the crack tip, highlighting both its role in significantly limiting crack velocities and its 3D nature. We then show that when micro-branching is suppressed by approaching the 2D limit, cracks accelerate to extremely high velocities, where they become unstable to spontaneous shape oscillations at extreme velocities. Recent theoretical and experimental developments have shed new light on the origin of this instability, and its relation to crack tip nonlinearities through an intrinsic length scale.

The results discussed in Sects. 2–4 mainly focus on cracks that propagate in an effectively 2D medium. Section 5 discusses phenomena that entail an intrinsically 3D description of fracture dynamics. Based on very recent experiments, we provide additional insight into the properties and origin of the micro-branching instability and provide evidence that it is related to the oscillatory instability. We then briefly discuss both in-plane and out-of-plane crack front dynamics.

While Sects. 2–5 consider cracks that are ostensibly tensile in nature, Sect. 6 briefly reviews studies that reveal relations between frictional motion and dynamic shear (mode II) cracks. Experiments over the last decade or so have revealed tight connections between interfacial friction dynamics and crack-like ruptures that appear similar to earthquakes along natural faults. Recent experiments, moreover, suggest that at least some of these can be described with classical mode II crack solutions. Understanding others requires richer coupling of bulk elasticity to constitutive descriptions of friction.

We conclude with some opinions on various directions in which the field of dynamic fracture may evolve in the future.

2 The equation of motion for simple cracks

What are "simple" cracks? Let us define a simple crack as a single crack that propagates along a single (straight) fracture plane (Bouchbinder et al. 2010a). A simple crack is, basically, a crack that does not undergo any path instabilities. How is the motion of such cracks described? The equation of motion for simple cracks is based on the principle of energy balance (Freund 1990; Broberg 1960; Kostrov 1975; Rice 1968b); the energy release rate G (the elastic energy released per unit crack surface) is balanced by the fracture energy Γ (the energy dissipation per unit crack surface).

As long as the surrounding material is elastic, Γ represents all of the energy dissipated by a crack. For brittle materials, the "small scale yielding" assumption is valid; all of the dissipative processes are encompassed in a sufficiently small region surrounding the crack tip (Freund 1990). $\Gamma(v)$ is, in general, a material function that may depend on the crack velocity, v (Irwin 1957; Bergkvist 1974; Dally 1979; Kobayashi and Mall 1978; Ravi-Chandar and Knauss 1984a; Rosakis and Freund 1981). Its v-dependence is often unknown, but in some cases can be measured (Sharon and Fineberg 1996; Goldman et al. 2010; Baumberger et al. 2006).

The other "leg" of the energy balance equation is the energy release rate, G. The latter is a property of the elastodynamic solution of a moving crack and can be obtained by the J-integral for steady-state cracks or more generally by the dynamic stress intensity factor. Within the framework of LEFM, the near tip stress $\boldsymbol{\sigma}$ (as well as displacement gradient) fields are characterized by a universal singularity, $\boldsymbol{\sigma} \sim K_{I,II}/\sqrt{r}$, where the intensity of the singularity is quantified by the stress intensity factors $K_{I,II}$. K_I corresponds to mode I frac-

ture, i.e. tensile cracks, and K_{II} corresponds to mode II fracture, i.e. shear cracks. The stress intensity factors depend on the loading configuration and geometry of a given fracture problem. Once they are known, the energy release rate G can be readily calculated. The equation of motion for a straight crack is then given by $\Gamma(v) = G$. Next, we briefly discuss two such equations, which were quantitatively tested in recent experiments.

The most well-known equation of motion was obtained for a finite crack propagating in an infinite medium. In this case, the equation takes the form (Freund 1990)

$$\Gamma(v) = G(l, v) \simeq \frac{\sigma_\infty^2}{E}\, l \left(1 - \frac{v}{c_R}\right), \qquad (1)$$

where a pre-factor of order unity was omitted. Here l is the crack length ($\dot{l} = v$), σ_∞ is the externally imposed tensile stress far from the crack, E is Young's modulus and c_R is the Rayleigh wave-speed. Once $\Gamma(v)$ is known, Eq. (1) is a first-order nonlinear evolution equation for $l(t)$. It is valid as long as "small scale yielding" conditions prevail (i.e. linear elasticity is valid everywhere except for a small region near the tip, the so-called process zone). Additionally, the externally applied stresses should be able to be mapped to tractions applied to the crack faces and the crack cannot interact with the external boundaries (i.e. it propagates in an effectively unbounded medium).

The most interesting properties of Eq. (1) are that the crack tip dynamics are not inertial, i.e. the tip behaves as a massless "particle" where the acceleration $\dot{v}$ plays no role (of course *material* inertia is essential for this equation to hold), and that the limiting propagation velocity is c_R. The equation has been shown to beautifully describe crack's motion when its underlying assumptions are met (Bergkvist 1974; Washabaugh and Knauss 1994; Sharon and Fineberg 1999; Kessler and Levine 2003; Miller et al. 1999). In particular, this description was shown to be valid in experiments in brittle acrylic, PMMA, for $v < 0.4c_R$ (when cracks are indeed simple) (Sharon and Fineberg 1999). More recent experiments showed the equation of motion to be in excellent quantitative agreement with measurements of dynamic cracks in brittle gels for an unprecedented range of velocities, $0 < v < 0.96c_R$, approaching the limiting velocity (Goldman et al. 2010). This wide velocity range was only accomplished by suppressing crack instabilities. This excellent agreement with theory, presented in Fig. 1, was obtained entirely from first principles with no adjustable parameters.

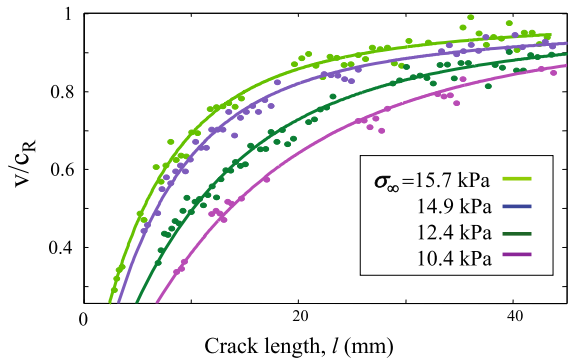

Fig. 1 The measured crack propagation velocity v as a function of the crack length l (*circles*) compared to the LEFM predictions in Eq. (1) (*solid lines*), for various values of the far field tensile stress $\sigma_\infty = 15.7, 14.9, 12.4, 10.4$ kPa (*top to bottom*). All measurements are for single cracks propagating in effectively "infinite medium" conditions ($l(t) < 2b = 125$ mm). Adapted from Bouchbinder et al. (2014)

Less known is an equation of motion for simple cracks which is valid when the crack "knows" about the external boundaries. While energy balance is always respected, Eq. (1) was derived for a system of infinite extent and, therefore, does not account for energy reflected back to the crack from external boundaries. When the waves that the crack emits during propagation are reflected back from the outer boundaries, the crack's dynamics may undergo a qualitative change. Let us consider the important particular case of a crack propagating in a long strip of width $2b$ which is loaded uniaxially by fixed tensile displacements. When the crack is sufficiently long, $l \gg b$, there is a fixed amount of strain energy per unit area W stored way ahead of the tip and no stored energy well behind the tip. Consequently, under steady state conditions the crack velocity is simply determined by $\Gamma(v) = W$. Marder derived the crack evolution approaching this steady state to leading order in the dimensionless acceleration $b\dot{v}/c_d^2$, where c_d is the dilatational wave-speed (Marder 1991). In this case, the crack length plays no role (the relevant length scale is b, not l), but the acceleration (which quantifies the deviation from steady state) is the relevant dynamical quantity. It is worth noting that this acceleration dependence is entirely due to the crack's interaction with the system boundaries and not to, for example, large acceleration corrections to the stress

fields predicted for rapidly accelerating cracks in an infinite system (Liu et al. 1993). This (little known) equation of motion takes the form (Marder 1991)

$$\Gamma(v) = G(v, \dot{v}) \simeq W \left[1 - \frac{b\,\dot{v}}{c_d^2} \left(1 - \frac{v^2}{c_R^2} \right)^{-2} \right] . \quad (2)$$

This equation is qualitatively different from Eq. (1) in one major aspect: the crack tip dynamics are effectively inertial, involving acceleration and an "effective mass" proportional to $(1 - v^2/c_R^2)^{-2}$, rather than being "massless" as in Eq. (1). These effective inertial dynamics are inherited from the interaction of the crack with the strip boundaries (and hence with its own history, giving rise to "memory"). Since W is externally controlled and $\Gamma(v)$ is a bounded material function (attaining a finite value as $v \to c_R$), one can impose $W > \Gamma(c_R)$. In this case, the divergence of the effective mass proportional to $(1 - v^2/c_R^2)^{-2}$ as $v \to c_R$ ensures that c_R is still the limiting velocity as in Eq. (1) (here $\dot{v} \to 0$ such that $\dot{v}(1 - v^2/c_R^2)^{-2}$ remains finite as $v \to c_R$). The predictions of Eqs. (1) and (2) can be tested in a single experiment involving a long strip under fixed displacement boundary conditions. For short times and $l(t) \ll b$, we expect Eq. (1) to be valid, while for longer times and $l(t) \gg b$, we expect Eq. (2) to be valid, with some crossover in between. A comparison to such an experiment, shown in Fig. 2, demonstrates that both Eqs. (1) and (2) are quantitatively correct when valid and that the transition between them is rather sharp.

Therefore, while for many the equation of motion described by Eq. (1) is unjustifiably thought to be universal, Eq. (2) explicitly demonstrates that this is not the case. In fact, we fully expect that the qualitative dynamics which are inherent in Eq. (2) are in many ways general. If, for whatever reason, a crack is allowed to interact with its history, we should expect strong memory, inertial-like, effects. Examples where such interactions may occur are when a crack tip/front encounters a localized inhomogeneity or obstacle in its path. In such cases, when the translation invariance along the singular crack front—the crack's leading *edge* in 3D—is broken, it has been shown that waves will propagate along the crack's front (Ramanathan and Fisher 1997; Morrissey and Rice 1998, 2000; Sharon et al. 2001, 2002; Sagy et al. 2002, 2004). These waves, which transfer energy between different points along the crack front,

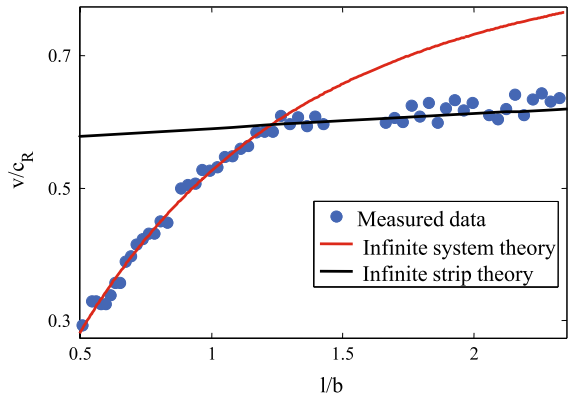

Fig. 2 The measured crack velocity versus crack length in a sample of dimensions $120 \times 30 \times 0.2$ mm (*circles*) compared to the LEFM prediction for an infinite medium [small $l(t)$], Eq. (1) (*red line*), and to the LEFM prediction for an infinite strip [large $l(t)$], Eq. (2) (*black line*). The rather sharp transition between the two regimes occurs at $t \sim 2b/c_s$ (b is the half-width of the strip and c_s is the shear wave-speed), when reflected waves from the vertical boundaries interact with the crack tip. Adapted from Goldman et al. (2010)

may influence crack dynamics in much the same way that the reflected waves that lead to Eq. (2) impart a crack with inertia. Moreover, experiments have shown that the crack front indeed retains a memory of an obstacle after it has passed it; damped oscillations of the front are observed immediately in the wake of a localized obstacle (Sharon et al. 2002). These issues will be briefly discussed in Sect. 5.

3 Weakly nonlinear theory of fracture, near-tip fields and intrinsic length scales

The equations of motion for simple cracks, which were discussed above, are based on energy balance. We would like now to consider the actual fields that mediate the transport of energy to the crack tip region and may control the fracture process itself. LEFM predicts that sufficiently close to the crack tip the stress field features a universal square-root singularity, $\boldsymbol{\sigma} \sim 1/\sqrt{r}$, where the pre-factor incorporates a universal tensorial function of the angle θ and the propagation velocity v (r and θ are polar coordinates co-moving with the tip), and the scalar multipliers—the stress intensity factors. Due to linearity, the displacement gradients feature the same singularity $\nabla \boldsymbol{u}^{(1)} \sim 1/\sqrt{r}$, where $\boldsymbol{u}^{(1)}$ is the linear elastic displacement field.

The LEFM fields possess certain peculiar features that are worthwhile noting. For example, in mode I (tensile) fracture, the crack parallel component of the stress tensor ahead of the tip, $\sigma_{xx}(r, \theta = 0, v)$, is *larger* than the tensile component $\sigma_{yy}(r, \theta = 0, v)$ for every finite crack velocity $v > 0$ (Rice 1968a; Langer and Lobkovsky 1998; Fineberg and Marder 1999). In fact, the ratio $\sigma_{xx}(r, \theta = 0, v)/\sigma_{yy}(r, \theta = 0, v)$ diverges as $v \to c_R$. This feature implies that it is not easy to explain why mode I cracks propagate perpendicularly to the tensile loading (y) axis based on the LEFM universal fields. While this feature has been recognized in the past, it has not received much attention. A corollary of this is that there always exists a crack propagation velocity $v_0 = \frac{1}{2}\left(\sqrt{c_d^2 + 8c_s^2} - c_d\right)$ [cf. Eq. (49) in Bouchbinder et al. (2014) and note that c_s is the shear wave-speed] above which $\partial_y u_y^{(1)}(r, \theta = 0, v)$ becomes *negative*. That is, the universal LEFM fields predict that tensile cracks, which ultimately involve extending—and eventually breaking—bonds ahead of their tips, propagate with a predominantly compressive displacement gradient ahead of their tip (Livne et al. 2010).

These features suggest that the LEFM universal fields are insufficient to fully explain the fracture process, an observation supported by explicit measurements of the strain fields surrounding dynamic cracks (Livne et al. 2008). This by no means implies that LEFM is wrong, this theory accurately predicts the flux of energy into the tip region and the universal LEFM fields pose the proper boundary conditions on any inner problem which is defined inside the process zone. It does imply, though, that the *length scale* at which these fields are valid is quite distinct from the scale where fracture actually takes place. LEFM, however, is a scale-free theory that provides no specific information about where it is valid and on what length scale it breaks down. This issue of the absence of an intrinsic length scale may have serious consequences in the context of dynamic instabilities, as will be discussed below.

Recently, these issues have been addressed in the framework of the "Weakly nonlinear theory of fracture" (Bouchbinder et al. 2008, 2009, 2010b, 2014; Bouchbinder 2010). This theory is based on a general expansion of the strain energy functional U in the form

$$U(\boldsymbol{E}) \simeq \frac{\lambda}{2}(tr\boldsymbol{E})^2 + \mu\, tr\boldsymbol{E}^2 + \beta_1 (tr\boldsymbol{E})^3 + \beta_2 tr\boldsymbol{E}\, tr\boldsymbol{E}^2 + \beta_3 tr\boldsymbol{E}^3 + \mathcal{O}(\boldsymbol{E}^4), \quad (3)$$

where $\boldsymbol{E} = \frac{1}{2}[(\nabla\boldsymbol{u}) + (\nabla\boldsymbol{u})^T + (\nabla\boldsymbol{u})^T(\nabla\boldsymbol{u})]$ is the nonlinear Green–Lagrange strain tensor (Holzapfel 2000) and $\boldsymbol{u}$ is the displacement field. Here λ and μ are the standard Lamé (second order) constants and $\{\beta_1, \beta_2, \beta_3\}$ are the third order elastic constants (Murnaghan 1951), which are basic physical quantities that are related to the leading anharmonic contributions to the interatomic interaction potential. The third order elastic constants are not free parameters, but rather quantities that are either calculated from a fully nonlinear elastic energy functional, if known, or measured directly in experiments (Bouchbinder et al. 2014).

As is evident from Eq. (3), the weakly nonlinear theory takes into account the leading elastic nonlinearities when LEFM breaks down. The basic idea is that in the presence of the intense displacement gradients near crack tips in brittle materials, linear elasticity first gives way to nonlinear elasticity, rather than to dissipation. As such, it is an asymptotic (in space, where LEFM breaks down near the tip of a crack) and perturbative (in the magnitude of displacement gradients) theory based on the expansion $\nabla\boldsymbol{u} = \nabla\boldsymbol{u}^{(1)} + \nabla\boldsymbol{u}^{(2)} + \mathcal{O}(|\nabla\boldsymbol{u}^{(3)}|)$, where the superscripts denote different orders in the displacement gradients. $\boldsymbol{u}^{(1)}$ simply corresponds to LEFM and $\boldsymbol{u}^{(2)}$ satisfies a new equation that depends both on the nonlinearity and $\boldsymbol{u}^{(1)}$. The solution to this equation takes the form (see details in Bouchbinder et al. 2014)

$$u_x^{(2)} \sim \frac{K_{I,II}^2}{\mu^2}\left[\log r + f_x^{I,II}(\theta, v)\right],$$
$$u_y^{(2)} \sim \frac{K_{I,II}^2}{\mu^2} f_y^{I,II}(\theta, v) \quad (4)$$

and is inherently mode I (tensile) for $\boldsymbol{u}^{(1)}$ corresponding to *both* mode I *and* mode II. That is, the explicitly calculable functions $f_{x,y}^{I,II}(\theta, v)$ satisfy $f_x^{I,II}(\theta, v) = f_x^{I,II}(-\theta, v)$ and $f_y^{I,II}(\theta, v) = -f_y^{I,II}(-\theta, v)$. Note that r inside $\log r$ in Eq. (4) should be made non-dimensional, but this simply adds a constant and is not included here.

The theory, as is clearly observed in Eq. (4), predicts a stronger than $1/\sqrt{r}$ divergence of the displacement gradient tensor field, $\nabla\boldsymbol{u}^{(2)} \sim 1/r$, and a logarithmic stretching of the crack tip opening displacement, which is strictly parabolic in LEFM (Freund 1990). This $1/r$ displacement gradient singularity has a fundamentally different status compared to apparently similar singularities in LEFM (Hui and Ruina 1995; Williams 1957). In particular, its contribution to the J-

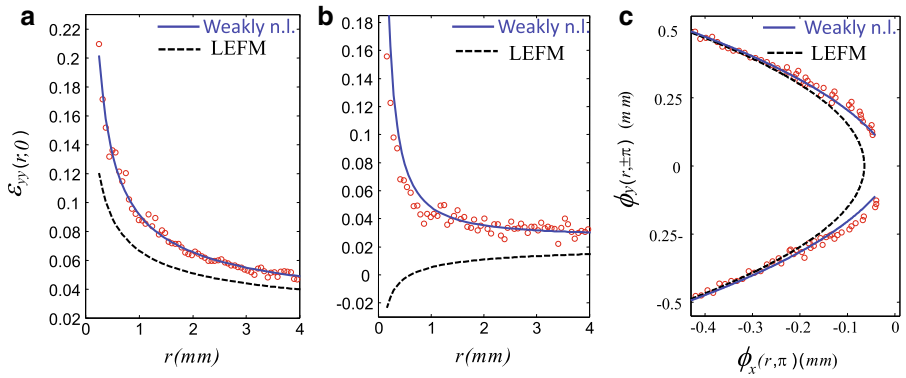

Fig. 3 **a** The measured yy-component of the displacement gradient tensor $\varepsilon_{yy}(r,\theta=0)=\partial_y u_y(r,\theta=0)$ ahead of a crack propagating at $v=0.20c_s$ (*circles*) compared to the LEFM prediction (*dashed line*) and the weakly nonlinear theory prediction [LEFM supplemented with Eq. (4)]. **b** The same for $v=0.78c_s$. Note, in particular, that for $v>v_0=0.73c_s$, LEFM predicts $\varepsilon_{yy}(r,\theta=0)<0$ sufficiently close to the tip, while both the experiment and the weakly nonlinear theory show that $\varepsilon_{yy}(r,\theta=0)>0$, as is physically expected in mode I fracture. **c** The measured crack tip profile ($\phi_y(r,\theta=\pm\pi)$ versus $\phi_x(r,\theta=\pi)$ for $v=0.53c_s$, where $\boldsymbol{\phi}(\boldsymbol{x})\equiv\boldsymbol{x}+\boldsymbol{u}(\boldsymbol{x})$ (*circles*) compared to the best fit of the parabolic LEFM profile (*dashed line*) and that predicted by the weakly nonlinear theory (*solid line*). The effect of the logarithmic stretching term in Eq. (4) is evident as the tip is approached. Adapted from Bouchbinder et al. (2008), where additional details can be found

integral vanishes identically. This, and other properties, are discussed in detail in Bouchbinder et al. (2009, 2014). These predictions were quantitatively verified by direct experiments on rapid cracks, as shown in Fig. 3. In particular, it is explicitly shown (panel b) that for a propagation velocity for which LEFM predicts a negative displacement gradient $\partial_y u_y^{(1)}(r,\theta=0,v)<0$ near the tip (i.e. $v>v_0$, where in this case $v_0=0.73c_s$), both the experimentally observed and theoretically predicted $\partial_y u_y(r,\theta=0,v)$ are positive, the latter *directly* due to the nonlinear contribution $\partial_y u_y^{(2)}(r,\theta=0,v)$.

To sum up, the weakly nonlinear theory of fracture—and its experimental verification—show that elastic nonlinearities give rise to a stronger near tip singularity compared to LEFM and to an extensional displacement gradient ahead of the tip, $\partial_y u_y(r,\theta=0,v)>0$, even at propagation velocities where LEFM predicts otherwise (i.e. for $v>v_0$, cf. Fig. 3b). The latter at least recovers the basic physical intuition that mode I fracture occurs under extensional deformation ahead of the propagating tip. As was mentioned above, when nonlinearities are taken into account for mode II cracks (Harpaz and Bouchbinder 2012), a symmetry-breaking effect in which LEFM mode II (shear) cracks feature mode I (tensile) properties naturally emerges in this theoretical framework (Stephenson 1982).

As the weakly nonlinear theory features two different singularities associated with two different constitutive relations, it predicts the existence of a new intrinsic (i.e. non-geometric) length scale, ℓ_{nl}, which characterizes the scale at which the two singular solutions are comparable in magnitude, i.e. roughly when $|\nabla\boldsymbol{u}^{(1)}|\simeq|\nabla\boldsymbol{u}^{(2)}|$. This intrinsic length scale is a dynamic quantity (i.e. it exhibits a non-trivial velocity dependence) that depends on the third order elastic constants. Its length dimension is inherited from Γ/E, i.e. $\ell_{nl}\propto\Gamma/E$, with a nontrivial and not necessarily order unity pre-factor. Finally, we note that very recently an Extended Finite Element Method (XFEM) analysis of nonlinear fracture problems based on the weakly nonlinear theory has been performed (Rashetnia and Mohammadi 2015). It was shown that using the analytic properties of the solution in Eq. (4) to construct crack tip enrichment functions provides an accurate and efficient tool for solving finite strain fracture problems.

The weakly nonlinear theory of fracture, which invokes three directly measurable third order elastic constants, provides a general and systematic way to go beyond LEFM at smaller scales near the tip. It naturally resolves apparently paradoxical physical features of the LEFM universal fields and gives rise to a new intrinsic length scale, which is missing in LEFM. As will be discussed soon, the latter plays an important role in dynamic instabilities.

4 Crack instabilities

4.1 The micro-branching instability

Historically, early measurements showed that a running crack did not seem to be described by the equations of motion described in Sect. 2. In particular, these measurements suggested that even as robust a prediction as the limiting velocity of a dynamic crack seemed to be off; cracks in brittle materials rarely surpassed even 60 % of c_R. These observations suggested that something was seriously wrong with our fundamental understanding of rapid crack dynamics, but it was unclear where the root of the problem lay. One could always "blame" the velocity dependence of the fracture energy, $\Gamma(v)$, but then one had to explain why, in brittle amorphous materials $\Gamma(v)$ needed to increase precipitously in order to prevent Eq. (1) from allowing a crack to approach c_R. Even more puzzling was the fact that this behavior occurs in a variety of materials whose molecular dissipative mechanisms are expected to be wholly unrelated; these materials ranged from brittle (cross-linked and uncross-linked) polymers to glasses.

The answer to the apparent paradox suggested above is that at high velocities, the crack is no longer a "simple crack". Instead, as first observed in Ravi-Chandar and Knauss (1984a, b), a crack's structure at relatively high propagation velocities is entirely different from that envisioned in the picture of simple crack; high-speed photographs of rapid cracks showed that the structure of the crack tip was anything but simple. Instead of the propagation of a single simple crack, these experiments showed that rapid cracks are composed of an ensemble of simultaneously propagating cracks. Later experiments (Fineberg et al. 1991), suggested that the break-up of a simple crack to multiple cracks occurred at a critical velocity, at which a single crack became unstable. This instability, which became known at the "micro-branching" instability, was later shown to be characteristic of many brittle amorphous materials (Fineberg and Marder 1999; Ravi-Chandar and Knauss 1984a; Fineberg et al. 1991; Cramer et al. 2000; Sharon and Fineberg 1998, 1996; Gross et al. 1993; Sharon et al. 1995; Boudet et al. 1995; Livne et al. 2005; Yang and Ravi-Chandar 1996; Ravi-Chandar and Yang 1997). A comprehensive review of some of the early work on the micro-branching instability can be found in Fineberg and Marder (1999).

What is the micro-branching instability? For low crack velocities, the crack propagates smoothly and the fracture surfaces formed are smooth and mirror-like, with the only apparent structure caused by material defects interacting with the singular front (Yang and Ravi-Chandar 1996; Scheibert et al. 2010). At a critical velocity of $v_{mb} \simeq 0.4c_R$, the crack undergoes a dynamic instability. As shown in Fig. 4, rapid fluctuations appear in the instantaneous crack velocity and, at the same time, non-trivial structure emerges on the fracture surface. The fracture surface structure is accompanied by frustrated crack-branching, as multiple microscopic crack branches ("micro-branches") are observed below the fracture surface. As the crack velocity increases beyond v_{mb}, both the length and density of the micro-branches increase with v. The increased length and density of the micro-branches gives rise to correspondingly rougher fracture surface features, larger velocity fluctuations, and a sharp increase of the fracture energy that is proportional to the total micro-branch length (Sharon and Fineberg 1996; Sharon et al. 1996). As Fig. 4 demonstrates, these characteristic features are independent of the brittle material; shown are two extremely different classes of material, poly-acrylamide gel (an aqueous elastomer) and soda-lime glass which exhibit identical characteristic behavior (Livne et al. 2005). Note the use of brittle gels has enabled experiments to probe the fracture process in unprecedented detail, as demonstrated in Fig. 5.

Over the past two decades, there have been a number of notable attempts to describe the micro-branching instability by supplementing or extending LEFM in various ways. These include phase-field models (Aranson et al. 2000; Karma and Lobkovsky 2004; Henry and Levine 2004; Henry 2008; Spatschek et al. 2006, 2011; Henry and Adda-Bedia 2013), phase transformation models (Fleck et al. 2011), cohesive-zone models (Miller et al. 1999; Langer and Lobkovsky 1998; Falk et al. 2001), lattice models (Holland and Marder 1999; Slepyan 2002; Marder and Liu 1993; Marder and Gross 1995; Heizler et al. 2002; Kessler and Levine 2001; Guozden et al. 2010), models based on the "Principle of Local Symmetry" (Adda-Bedia et al. 1999; Movchan 2005; Bouchbinder and Procaccia 2007), energetic bounds on crack branching (Eshelby 1971; Adda-Bedia 2005; Bouchbinder et al. 2005) and models based on non-linear constitutive behavior near the crack tip (Gao 1996; Buehler and Gao 2006; Bouch-

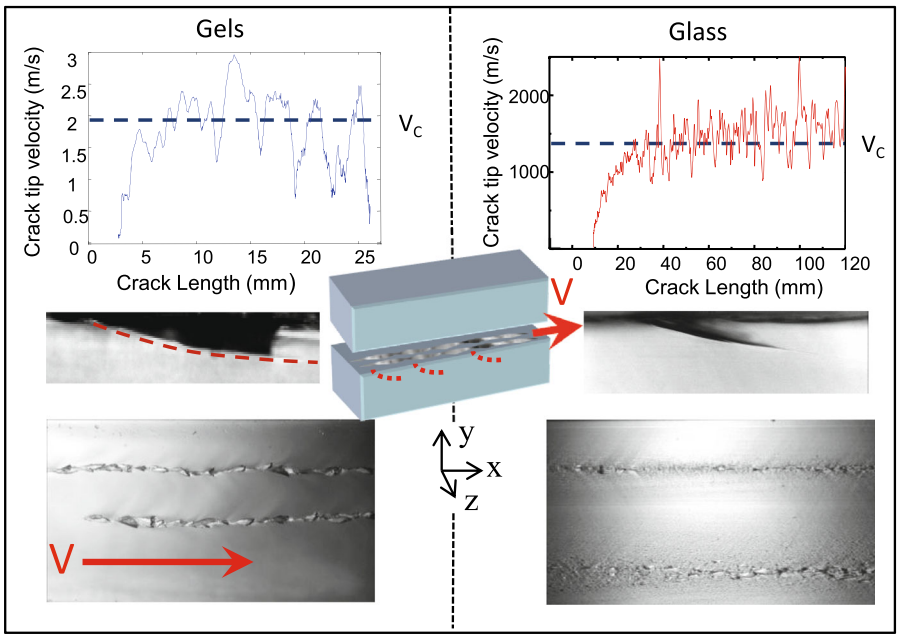

Fig. 4 A comparison between the instability in both soft polyacrylamide gels (*left*) and soda-lime glass (*right*). Once a crack attains a critical velocity of $v \simeq 0.4c_R$, a single "simple" crack may become unstable to the micro-branching instability. At this point (*top*) the instantaneous velocity of the crack undergoes violent oscillations that correspond to the formation of subsurface frustrated micro-branches (*center*), where side views (xy plane) of micro-cracks in both materials are presented (x is the propagation direction, y is the loading direction and z is the direction along the crack front). Micro-branches are very similar in both materials, characterized by a power-law functional form. *Bottom* photographs of the resulting fracture surface (xz plane) formed by cracks propagating from left to right at $v \simeq 0.5c_R$. The chains of structures on the fracture surface correspond to chains of micro-branches that are aligned in the propagation direction x and highly localized in the z direction. The *vertical dimensions* of the photographs are about 0.5 mm. The cartoon in the center describes the geometry; the xz fracture surface is formed by a propagating cracks whereas micro-branches (*dotted lines*) extend below the surface. Adapted from Bouchbinder et al. (2014)

binder 2009). Although many of these models exhibited some properties that were qualitatively consistent with the experimental observations, they are inherently deficient because they focussed on 2D (i.e. they actually studied macro-branching, which appears as a tip-splitting instability). As will be shown below, micro-branching appears to be an intrinsically 3D instability that cannot be satisfactorily described as a 2D phenomenon.

On the conceptual level, we note that most of previous works have considered the near-tip region as a passive region that both regularizes the singular fields predicted by LEFM and accounts for the dissipative processes at the tip, but otherwise plays no other active role in the dynamics. As will be shown next, recent developments may suggest that understanding crack instabilities may entail the introduction of new physical ingredients (e.g. length scales) in which the near-tip region plays a more active role.

4.2 The oscillatory instability

By manipulating the geometry and thickness of the brittle gels mentioned above, it is possible to statistically suppress the micro-branching instability in sufficiently thin samples (200–300 μm) (Livne et al. 2007; Goldman et al. 2012); while micro-branching can occur for *all* velocities $0.3c_s < v < 0.9c_s$, the probability of exciting them decreases for both thin samples and large crack accelerations. When micro-branching is suppressed, simple brittle cracks can reach extreme velocities. In such cases single crack dynamics, as described by LEFM (Fig. 1), can be obtained for velocities approaching c_R.

Can these cracks actually reach their asymptotic velocity? It turns out that this is prevented by a *new* instability. Experiments in gels have found that at velocities surpassing about 90 % of the shear wave-speed, c_s, a straight crack becomes unstable to sinu-

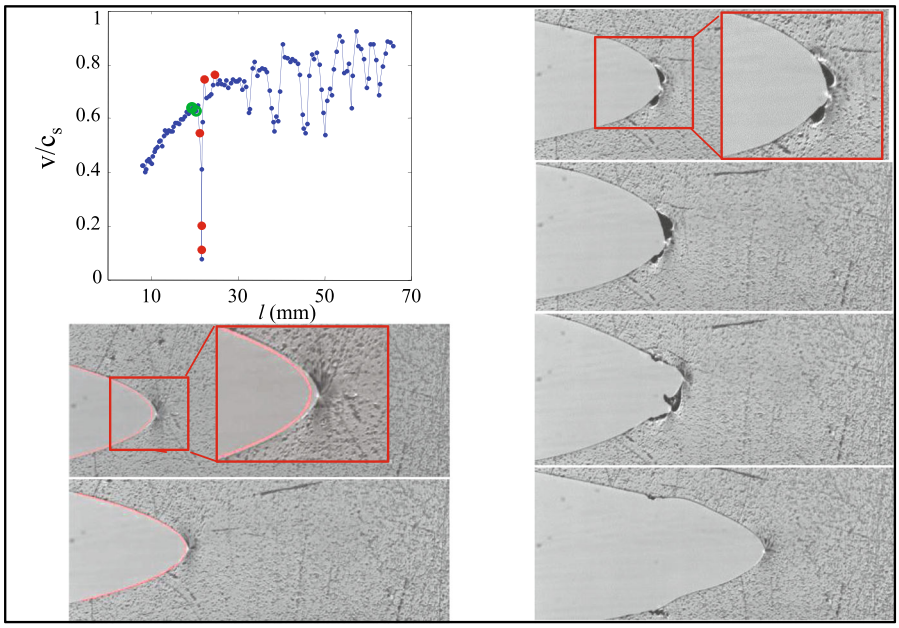

Fig. 5 A series of photographs of the quasi-parabolic profile of running cracks in polyacrylamide gels. The two *lower left panels* depict the parabolic crack tip opening profile of "simple" cracks propagating just prior to the onset of the micro-branching instability (corresponding to the *green dot* on the velocity vs. crack length figure in the *upper right corner*). *Right panels* 4 profiles of cracks undergoing the micro-branching instability, corresponding to the *red dots* in the velocity measurements. Note the small micro-cracks formed at the tip of the main crack. Adapted from Bouchbinder et al. (2014)

soidal path oscillations (Livne et al. 2007). This instability is particularly intriguing since it involves a finite instability wavelength at onset whose value was not dependent on either the system geometry or the loading conditions. This suggests the existence of an intrinsic scale that can not exist in linear elastic solutions for cracks, which are scale-free.

This oscillatory instability should be distinguished from apparently similar oscillatory cracks observed in rubber (Deegan et al. 2002). The oscillatory cracks in rubber were intersonic ($c_s < v < c_d$) (Marder 2006), entailed bi-axial loading, and were subjected to very large background strains (which make the material response nonlinear everywhere). The oscillatory cracks in the elastomer gels were subsonic and were observed under uniaxial loading of such magnitude ($\sim$10 %) that the deformation away from the tip was predominantly linear elastic.

4.3 Understanding 2D instabilities

In Sects. 2 and 3 we discussed simple tensile cracks that propagate along straight paths in effectively 2D bodies. By so doing, we excluded spontaneous symmetry-breaking instabilities from the discussion. Such dynamic instabilities, however, are rather prevalent and pose some of the most intriguing open questions in the field of dynamic fracture. In Sects. 4.1 and 4.2 we described two different instabilities that take place in fast fracture.

The oscillatory instability described in Fig. 6 is, in a sense, the simpler of the two instabilities. Once excited, the oscillatory instability breaks the translational invariance of a crack in the propagation (x) direction. The fracture surface created during the crack's motion is wavy but mirror-like; there is no apparent structure along the fracture surface. Thus, we can consider the crack front to be translationally invariant along the direction transverse (z direction) to the crack's propagation direction. It is, therefore, sufficient to idealize the crack tip as an oscillating point within an effectively 2D medium.

In contrast to the oscillatory instability, when the micro-branching instability is excited, distinct structures are generated along the fracture surface that are highly localized along both the x and z directions (see, for example, the lower panels of Fig. 4). As the crack front is *not* translationally invariant along the z

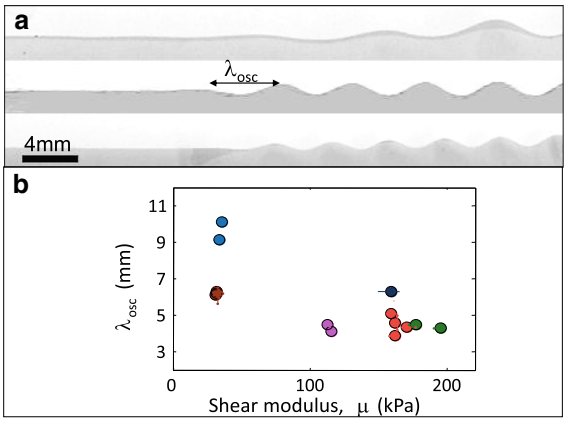

Fig. 6 **a** Typical photographs of the xy profiles of fracture surfaces at the onset of the oscillatory instability; from *top to bottom* gels with shear moduli $\mu = 36, 143, 168$ kPa. **b** The oscillation wavelength, λ_{osc} changes significantly with the material, as characterized by μ. *Symbol colors* as in **b**. Adapted from Goldman et al. (2012)

direction, it may not be sufficient to consider a crack propagating within a 2D medium to understand microbranching.

We now consider the oscillatory instability in a 2D medium. As mentioned above, the most interesting physical property of this instability, beyond its existence, is that its wavelength does not scale with the geometric dimensions of the sample. This implies that it cannot be explained by LEFM, as it possesses no intrinsic length scale beyond geometric length scales. What is then the origin of this instability and the emerging intrinsic length scale?

To address this question, and dynamic fracture instabilities in a broader context, we need to consider first a basic aspect of the current theoretical status of the field. When cracks propagate along straight paths (or other predetermined paths), the quantity of interest is the rate of crack growth, which involves a scalar relation based on energy balance. In the most general case, however, the path is an intrinsic property of the dynamic fracture problem and is selected self-consistently as in a large class of moving free-boundary problems (see, for example, Fineberg and Steinberg 1987; Saarloos 2003; Cross and Hohenberg 1993; Ebert et al. 1997; Sivashinsky 2002; Krug and Spohn 1991). Consequently, we need an equation of motion for crack tips (in 2D) and crack fronts (in 3D) that will allow the determination of both the direction of propagation and its rate. Such equations are intrinsically non-scalar in nature and involve physics that go significantly beyond energy balance alone. In particular, such equations are essential in the context of instabilities as without them one cannot even mathematically pose the question of stability, which amounts to perturbing solutions of existing and well-defined differential equations. We currently lack well-established crack tip/front equations of motion for general, non-straight, dynamics.

In 2D and under quasi-static conditions, $v \ll c_R$, it has been shown that the Principle of Local Symmetry (Goldstein and Salganik 1974) offers good approximations for crack paths (Cotterell and Rice 1980; Adda-Bedia and Pomeau 1995; Bouchbinder et al. 2003; Pham et al. 2008; Corson et al. 2009; Hakim and Karma 2005, 2009). This approximation suggests that under quasi-static conditions, and under the assumption that no intrinsic length scales exist near the tip, crack propagation along smooth paths will annihilate any shear (mode II) component of the fields ahead of the tip. Hence, this path selection criterion proposes that conditions of local tensile symmetry are almost maintained at a crack's tip, which mathematically amounts to $K_{II}/K_I \ll 1$. As the stress intensity factors are generically non-local functionals of the path, the latter is in fact an integro-differential equation. At present, to the best of our knowledge, there is no evidence that the Principle of Local Symmetry offers good approximations also under fully dynamic conditions. In fact, some recent experiments might indicate otherwise (Goldman Boué et al. 2015a).

Recently, a dynamic crack tip equation of motion, which takes into account the existence of an intrinsic length scale ℓ_{nl} and the possible high propagation velocities, was proposed (Bouchbinder 2009). The basic idea is that in the presence of a finite length scale ℓ_{nl} near the tip, causality implies a time delay between the singular fields driving the crack (as described by LEFM) and the actual crack tip. Taking into account this time delay along with scaling arguments and symmetry considerations (Hodgdon and Sethna 1993), a dynamic crack tip equation of motion has been constructed (Bouchbinder 2009).

This equation was used to study the linear stability of straight crack propagation against sinusoidal perturbations, with the help of the Willis–Movchan perturbation theory for the stress intensity factors (Willis and Movchan 1995, 1997; Obrezanova et al. 2002). This analysis predicted an oscillatory instability of mode I cracks to infinitesimal out-of-plane perturba-

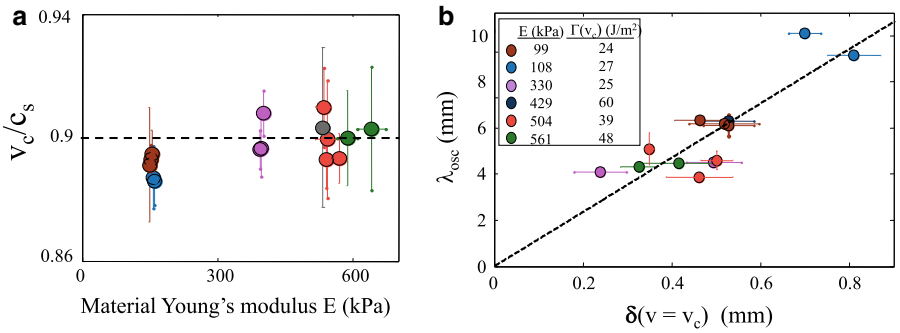

Fig. 7 **a** The scaled critical velocity for the onset of the oscillatory instability, $v_c/c_s \approx 0.9$, is constant. v_c is defined as the maximal velocity prior to the instability onset in each material. *Symbol colors* correspond to the legend in **b**. **b** Comparison between an experimental measure of the length scale associated with elastic nonlinearities $\delta(v_c)$ [measured at the critical velocity v_c, see Goldman et al. (2012) for details] and the oscillation wavelength λ_{osc}. Note that the different combinations of μ and Γ are used to produce these 15 independent measurements. The *dashed line* is a guide to the eye. Adapted from Goldman et al. (2012)

tions above a high propagation velocity of $v_c \simeq 0.8c_s$, with the following properties: (i) The normalized critical velocity v_c/c_s is nearly universal (it exhibits a weak dependence on Poisson's ratio ν), (ii) The wavelength of oscillation is proportional to the intrinsic length scale $\ell_{nl} \propto \Gamma(v_c)/E$ (Goldman et al. 2012). These predictions were recently tested by extensive experiments in which Γ and E were varied over a substantial range (Goldman et al. 2012). As Fig. 7 shows, a favorable agreement between theory and experiments was demonstrated.

We believe that these results are important because they show that the process zone is not a passive region responsible only for nonlinearity and energy dissipation, but rather an active region whose accompanying length and time scales can significantly affect macroscopic fracture dynamics, in particular crack instabilities. The importance of a length scale proportional to Γ/E has also been highlighted in experiments on the quasi-static fracture of hydrogels, where it was shown to play a decisive role in a mode I cross-hatching instability (Baumberger et al. 2008), in a wetting-induced branching instability (Baumberger and Ronsin 2010) and in a mixed-mode I+III (mode III corresponds to anti-plane shear fracture) échelon instability (Ronsin et al. 2014). We suspect that the incorporation of intrinsic length scales into fracture theory may be essential to developing equations of motion for crack tips/fronts and to understanding dynamic instabilities. Whether or not these ideas are also relevant to the crack oscillations observed in rubber (Deegan et al. 2002; Marder 2006; Chen et al. 2011), where the applied strains are extremely large and intersonic propagation velocities were reached, remains an open question.

5 Three-dimensional tensile cracks: Micro-branching, front waves and corrugations

In the previous section we discussed a way to understand the oscillatory instability based on a dynamic crack tip equation of motion that takes into account the length scale proposed by the weakly nonlinear theory of fracture mechanics. It was shown that a crack propagating in a 2D medium will lose its stability at extremely high velocities ($\sim 0.9c_s$) to infinitesimal out-of-plane perturbations. We are still faced, however, with the challenge of explaining the micro-branching instability. Micro-branching, on the face of it, appears to be a much more difficult problem. Once excited, this instability appears to be intrinsically 3D, as Fig. 5 suggests. It had been discovered in earlier work (Livne et al. 2005) that the micro-branching threshold, v_{mb}, could vary above a *minimum* value of about $v_{mb} \simeq 0.35c_R$. The observed values of v_{mb} were shown to statistically depend on the value of the acceleration prior to the instability initiation. In addition, the transition to micro-branching was observed to be hysteretic in v.

These observations suggested that the micro-branching instability involves an activated process that could be triggered by noise above the minimum value of v_{mb}. If the acceleration is low, micro-branching is always observed near the minimal value of v_{mb}, as eventually the crack front will encounter a noise

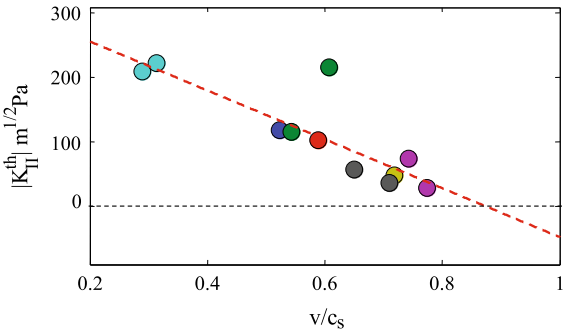

Fig. 8 Phase diagram of the micro-branching instability. The micro-branching instability is triggered when a small K_{II} component is present. For each propagation velocity v, there exists a threshold value, $K_{II}^{th}(v)$. When $K_{II} > K_{II}^{th}(v)$ micro-branching is observed. Shown are values $|K_{II}^{th}/K_I|$,which are the values obtained for each v immediately prior to micro-branching. The critical boundary linearly extrapolates (*dashed line*) to zero at $v \simeq 0.87c_s$, the value of the measured threshold velocity for the onset of the oscillatory instability (Goldman et al. 2012). *Colors* denote different experiments. Adapted from Goldman Boué et al. (2015a)

source that is sufficiently large to trigger the instability. In very thin gel samples, where "sources of noise" along the z direction are geometrically reduced, and at high crack accelerations, micro-branching was seen to occur in a relatively large range of velocities, $0.35c_s < v_{mb} < 0.9c_s$. This is the reason that the oscillatory instability could be, at all, observed prior to the onset of micro-branching (Livne et al. 2007; Goldman et al. 2012).

Very recent experiments, however, suggest that the micro-branching instability may be closely related to the oscillatory instability (Goldman Boué et al. 2015a). These experiments directly measured the 2D strain fields surrounding the tips of rapidly moving cracks in thin gels, as these cracks approached the instability over a wide range of v_{mb} values. Prior to the onset of micro-branching, the cracks were "simple" so that the media could be considered as 2D. It was discovered that the strain fields of all of these simple cracks prior to the onset of the instability contained a fluctuating shear component that could be characterized by the textbook K_{II} fields (Freund 1990). Examining the value of K_{II} immediately prior to the instability onset, these studies showed that there exists a velocity-dependent threshold value, $K_{II}^{th}(v)$, for the onset of instability.

K_{II}^{th} as a function of v is presented in Fig. 8. The data, when extrapolated to $K_{II}^{th}(v) \to 0$, yield a zero threshold propagation velocity of $0.9c_s$, which is precisely the critical velocity for the onset of the oscillatory instability. Guided by local symmetry arguments (Goldstein and Salganik 1974), we would expect any finite K_{II} value to cause a crack to curve away from the initial symmetry axis imposed by the loading. The data therefore suggest that two distinct "phases" can coexist in a hysteretic region $0.3c_s < v < 0.9c_s$, where both straight cracks and cracks that locally curve out of the symmetry plane can be simultaneously stable. Local crack curvature will only occur upon a sufficiently large (finite) local shear perturbation, as shown in Fig. 8. Moreover, in this bi-stable region, both straight and curved cracks can coexist within different sections along the crack front. This bi-stability provides an explanation for the localized nature of the micro-branches in the z-direction. The bi-stability that enables this localization disappears at the critical velocity $0.9c_s$, where $|K_{II}^{th}| = 0$. At this point the entire crack front must coherently curve out of plane and the oscillatory instability ensues.

Insofar as propagation along the symmetry axis is concerned, it is clear that straight sections of the crack front will outrun the curved sections. As a result, we expect that the crack front will eventually revert to a single fracture plane, pinching off the curved section. This "frustrated curved section" is what we identify as a micro-branch beneath the fracture surface. Such a pinch-off scenario been recently observed experimentally by direct visualization of crack fronts in the xz plane as micro-branching takes place (Kolvin et al. 2015). The micro-branch locally delays the crack front causing local crack front curvature within the xz (fracture) plane. This initial in-plane curvature was seen to continually deepen, eventually developing into a cusp-like shape. Cusp formation within the fracture plane was coincident with the "death" of the micro-branch.

Micro-branching is, therefore, an intrinsically 3D instability that is intimately related to the crack front dynamics, and hence defies any attempt to understand it in a purely 2D framework. There are several other basic phenomena that necessitate a 3D framework of fracture dynamics. In the quasi-static regime, simulations coupled with analytic work (Lazarus et al. 2001, 2008; Lin et al. 2010; Gao and Rice 1989; Xu et al. 1994) has shed light on a crack front instability under mixed-mode I + III conditions. Recently, helical perturbations have been shown, in 3D simulations, to develop into segmented crack fronts (Pons and Karma 2010; Leblond et al. 2011, 2015). Related segmented crack front struc-

tures have been observed in mode I (Baumberger et al. 2008; Tanaka et al. 1998) and mixed-mode I + III fracture of both "standard" (Smekal 1953; Sommer 1969; Knauss 1970; Cooke and Pollard 1996; Hull 1997; Pham and Ravi-Chandar 2014) and soft materials (Ronsin et al. 2014).

In the dynamic regime, crack fronts were shown to support propagative modes along them. The most well-established of those are in-plane crack front waves, which were predicted through perturbative mode I numerical (Morrissey and Rice 1998, 2000) and analytic (Ramanathan and Fisher 1997) calculations in the late 1990's. In this case, the crack front is assumed to remain within its tensile symmetry plane, but to experience in-plane shape perturbations. In the framework of LEFM and a linear perturbation theory (Ramanathan and Fisher 1997; Morrissey and Rice 1998, 2000), perturbations to the crack front were shown to propagate along the front without attenuation (as long as Γ is independent of v) at nearly c_R, for any v.

Subsequent experiments on various amorphous brittle materials (Sharon et al. 2001, 2002; Sagy et al. 2002, 2004) indeed revealed the existence of localized modes that propagated along the crack front at nearly c_R, when triggered by an interaction with localized material inhomogeneities (asperities) or by spontaneously generated micro-branches. The experimentally observed propagative modes were different from the theoretically predicted in-plane front waves in two important aspects: (i) They featured an out-of-plane component, which left marks on the fracture surfaces and, in fact, enabled post-mortem measurements of crack front waves (in-plane perturbations do not leave any post-mortem fractographic signature), (ii) They were clearly nonlinear, exhibiting soliton-like properties (Sharon et al. 2001). While similar fracture surface markings can also be generated by the interaction of shear waves with moving crack fronts (Bonamy and Ravi-Chandar 2003; Sharon et al. 2004; Ravi-Chandar 2004), recent measurements in both brittle gels (Livne et al. 2005; Kolvin et al. 2015) and the rapid fracture of rock (Sagy et al. 2004, 2006) have strengthened the evidence for the existence of front waves in dynamic fracture.

Treating out-of-plane front perturbations is more difficult than in-plane ones because the front interacts with out-of-plane perturbations which are locked in the front's wake and because energy balance alone is insufficient to determine the front dynamics (information about the direction of propagation is essential as well, see discussion above on crack front equations of motion). Only very recently, based on the Willis–Movchan 3D LEFM linear perturbation formalism (Willis and Movchan 1997) and the Principle of Local Symmetry, has the out-of-plane stability of crack fronts been considered (Willis et al. 2012; Adda-Bedia et al. 2013). In particular, a minimal scenario in which linearly unstable out-of-plane crack front corrugations might emerge (above a critical front propagation velocity), has been discussed. Within this scenario, a critical velocity has been calculated as a function of Poisson's ratio and corrugations have been shown to propagate along the crack front at nearly the Rayleigh wavespeed (Adda-Bedia et al. 2013).

To linear order in the deviation from a straight crack front, in- and out-of-plane perturbations are decoupled. Taken together with the nonlinear nature of the experimentally observed front waves, nonlinear coupling between in- and out-of-plane front dynamics appears to be an essential next step. Due to the technical difficulties involved, numerical approaches such as phase-field models may be useful in achieving this (Pons and Karma 2010). In addition, the effect of going beyond the Principle of Local Symmetry, e.g. in the spirit of Bouchbinder (2009), should be systematically explored. Possible connections to the much studied problem of fracture surfaces roughness (Bonamy and Bouchaud 2011), where dynamic effects are traditionally neglected (Bouchaud et al. 2002), should also be investigated.

6 The dynamics of frictional interfaces: on the relation between friction and fracture, and more

In this section we describe recent work that suggests that our understanding of many aspects of "commonplace" friction may need to be re-examined. This work suggests that dynamic fracture processes play a major role in frictional motion—even when these processes appear to be extremely slow. The key to understanding how dynamic fracture comes into play is to consider the spatially extended interface that separates two bodies in frictional contact. In dry friction, this interface is composed of a large ensemble of rough and interlocking discrete contacts, whose total area of contact is orders of magnitude smaller than the nominal contact area of the contacting bodies (Bowden and Tabor 2001; Dieterich

and Kilgore 1996). In order for frictional motion to initiate, these contacts must be "broken" or rupture. As we know, fracture of a spatially extended entity is not simultaneous, but is generally mediated by crack-like fronts. Below, we describe observations of such rupture fronts, which will be shown to be closely related to classic dynamic shear (mode II) cracks. It is intuitively obvious that these rapid rupture modes are also closely related to earthquakes, which mediate the relative motion of frictionally coupled tectonic plates.

The failure of macroscopic frictional interfaces has for centuries been thought to be governed solely by "friction laws", with the classic example of Amontons-Coulomb law of friction $F_s = \mu_{s,d} F_n$, where F_s is the friction (shear) force and F_n is the normal force. The proportionality constant is either the static friction coefficient μ_s or the dynamic one μ_d, both are considered to be characteristic properties of the materials forming the frictional interface. This class of friction laws has been generalized to spatially varying and more physically faithful constitutive laws (Rice and Ruina 1983; Dieterich 1979; Marone 1998; Scholz 1998; Baumberger and Caroli 2006). The latter, termed rate-and-state friction laws, incorporate the effects of additional dynamic variables such as the local sliding velocity ("rate") and the local average contact lifetime ("state") on friction.

A new generation of experiments over the past decade has revealed that rapid rupture fronts drive frictional motion. In other words, the transition from "static" to "dynamic" friction has been shown to be mediated by different types of crack-like fronts. These fronts are the vehicles that trigger the onset of macroscopic frictional motion, bridging the gap between the microscopic interactions that define local frictional resistance and the resulting macroscopic motion imbued in the slip of large bodies (Das 2003; Scholz 2002; Ben-Zion 2001, 2008). As shown in Fig. 9, these new experiments have revealed various rupture modes that are loosely classified as follows: slow ruptures, which propagate far below the material wave speeds (Rubinstein et al. 2004; Latour et al. 2013; Ben-David et al. 2010; Rubinstein et al. 2011), "sub-Rayleigh" ruptures (Rubinstein et al. 2004; Latour et al. 2013; Ben-David et al. 2010; Xia et al. 2004) that propagate up to the Rayleigh wave-speed c_R, and "super-shear" rupture modes that surpass the shear wave-speed c_s (Rubinstein et al. 2004; Ben-David et al. 2010; Xia et al. 2004; Scholz et al. 1972; Rosakis et al. 1999; Passelegue et al. 2013). It is important to note that analogs of all of these rupture modes have been documented in natural earthquakes (Ben-Zion 2001, 2008; Beroza and Ide 2011; Bhat et al. 2007; Robinson et al. 2006; Bouchon and Vallee 2003).

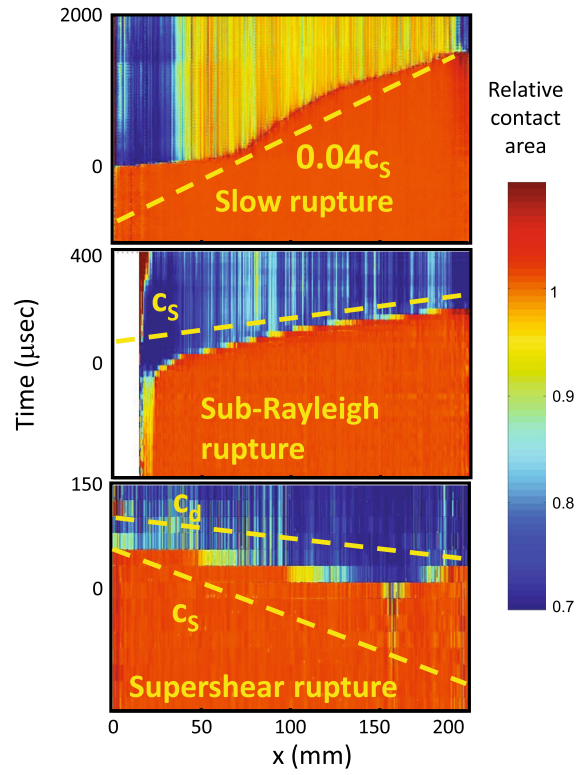

Fig. 9 Different types of rupture fronts in friction. Measurements of the real contact area reveal three qualitatively different types of fronts that "fracture" the contacts defining the interface that separates two sliding bodies. Shown is the space–time variation of the real area of contact along a 200 mm long frictional interface. The sharp reduction in the contact area occurs at the tip of the propagating fronts. Shown are typical examples of (*top*) slow (*center*) fast (*sub-Rayleigh*) and (*bottom*) supershear ($v > c_s$) fronts Adapted from Ben-David et al. (2010)

Are the rupture dynamics of an interface related to the values of the global "friction coefficients" that characterise the interface strength? Recent experiments using PMMA (Ben-David and Fineberg 2011) and granite (Passelegue et al. 2013) have measured the static friction coefficient, μ_s, i.e. the ratio between the applied shear and normal forces at the onset macroscopic sliding. These studies found, as shown in Fig. 10, that sliding can be initiated over a wide range of static friction values, indicating that μ_s is certainly not solely a characteristic material property but is, instead, dependent on how a given system is loaded (Ben-David and Fineberg 2011). Study of the rupture dynamics lead-

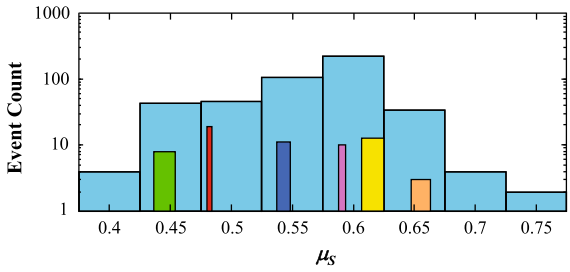

Fig. 10 Count of events with varying μ_s, from experiments conducted under widely varying loading conditions. These range from pure edge loading to near uniform application of the shear force, F_s, to the system. Note that this plot is *not* a histogram and solely reflects the number of experiments performed whose loading conditions yielded μ_s for each range. The *color bars* (bar width = two standard deviations) in the plot depict subpopulations of events from single experiments, each with different (specific) loading conditions. Adapted from Ben-David and Fineberg (2011)

ing to the broad range of friction coefficients, in fact, revealed that the loading conditions of the systems and the subsequent rupture dynamics were closely correlated to the value of μ_s (Ben-David and Fineberg 2011). These experiments found that μ_s was as well defined as the loading conditions. As long as the way in which forces were applied to two blocks in frictional contact was kept constant, μ_s was extremely well-defined. Once the loading configuration was changed, the measured value of μ_s for the *same* two blocks could be varied significantly and controllably, cf. Fig.10. This surprising result has been confirmed in recent theoretical and numerical studies (Tromborg et al. 2011; Kammer et al. 2012; Maegawa et al. 2010; Katano et al. 2014).

In addition to analytical work, recent numerical work (Tromborg et al. 2011; Kammer et al. 2012, 2015; Radiguet et al. 2013) together with simple models describing the contact dynamics of ensembles of discrete contacts have been successful in describing many aspects of frictional cracks (Rubinstein et al. 2011; Braun et al. 2009; Bouchbinder et al. 2011; Capozza and Urbakh 2012; Tromborg et al. 2014). These results have provided important new insights into the influence of both the discrete nature of the contacts that compose the frictional interface and the influence of different "friction laws" that couple the elastic medium to the interface.

How close to "ordinary" fracture might the rupture processes shown in Fig. 9 be? Let us consider two elastic bodies in frictional contact, subjected to remotely applied shear stresses. While in an intact homogeneous system the Principle of Local Symmetry would predict that any crack should rotate so as to annihilate any shear (mode II) component near its tip (Goldstein and Salganik 1974), the presence of a weak friction plane (compared to an intact bulk) allows rupture fronts to propagate under predominantly shear conditions along the weak plane. Are these rupture fronts related to classical mode II cracks? The surfaces left behind classical mode II cracks are assumed to be traction-free. While the propagation of rupture fronts along frictional interfaces is definitely accompanied by stress reduction ("stress drop"), it is clear that the frictional stress behind the propagating front is finite, and hence the physical situation is evidently different from the traction-free boundary conditions assumed in classical mode II crack solutions.

The two problems (i.e. of frictional rupture fronts and mode II cracks), though, are closely related when the following two conditions are met: (i) The residual stress σ_r left behind the rupture front is constant, a situation commonly assumed in the context of earthquake dynamics (Das 2003; Scholz 2002; Freund 1979; Burridge et al. 1979; Gabriel et al. 2013), (ii) The width of the front (the "cohesive zone"), i.e. the length scale over which the residual stress σ_r is reached when the front passes a point at the interface, is small compared to other length scales in the system. In particular, under these conditions the singular mode II fields of LEFM remain valid (in this case the singular K_{II} field mediates the transition from the initial shear stress to σ_r) (Palmer 1973; Rice 1980).

These predictions have been directly tested in very recent experiments on PMMA blocks, where the real-time strain tensor at points adjacent to the interface was measured during rupture propagation (Svetlizky and Fineberg 2014). In parallel, the instantaneous rupture tip location and velocity were measured. These techniques, which were used successfully to describe the strain fields in mode I fracture (Ravi-Chandar 1983), provided a first-time quantitative description of the strain fields surrounding the tips of these propagating rupture fronts. Measurements were performed for rupture fronts over a broad range of propagation velocities v, $0.04c_R < v < 0.97c_R$.

Typical results of these experiments are shown in Fig. 11, where a comparison of the different components of the strain tensor to the classic mode II singular solution for rupture fronts propagating at both slow velocities ($v < 0.3c_R$) and velocities approaching the

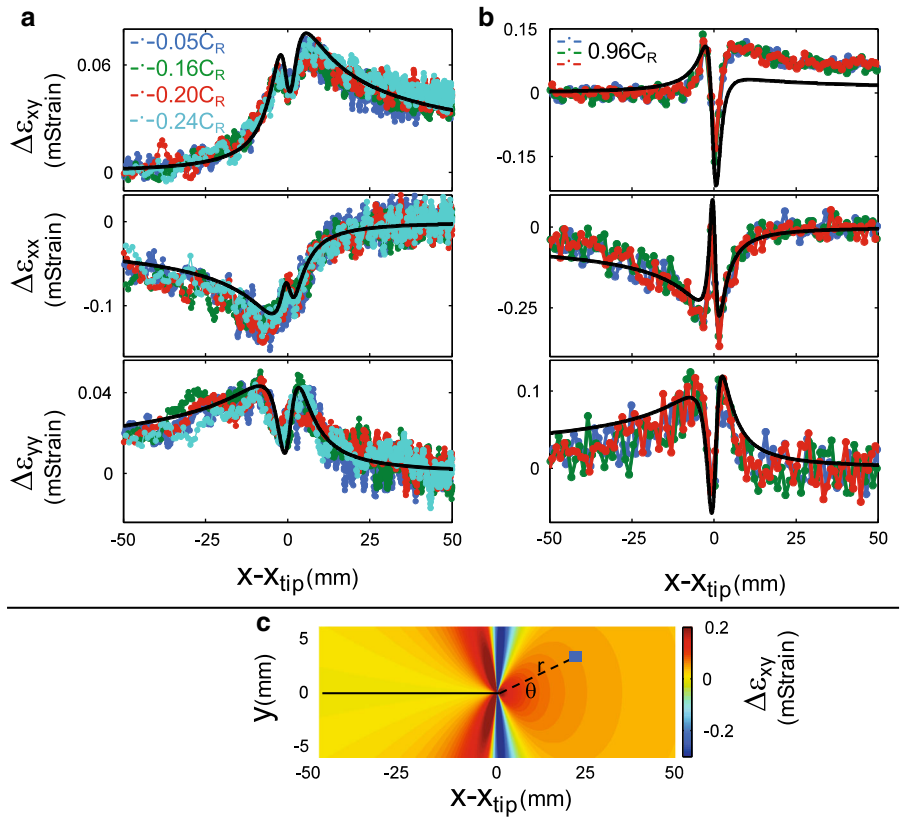

Fig. 11 **a** Measurements of the strain tensor, ε_{ij}, at a fixed spatial location above the frictional interface (see **c** for details) during the passage of a rupture front. The initial strain was subtracted from ε_{xx} and ε_{yy} and residual strain from ε_{xy}. *Colors* represent different, relatively small, front velocities ($0.05c_R < v < 0.24c_R$). Corresponding LEFM predictions for plain strain boundary conditions are *plotted in black* ($v = 0.2c_R$). The fracture energy $\Gamma \simeq 1.1\,\mathrm{J/m^2}$ is the sole free parameter. **b** ε_{ij} for $v \simeq 0.96c_R$. The LEFM solution (*black*), plotted as in **a**, still describes the larger amplitudes and strong oscillations of rapidly propagating ruptures with the *same* fracture energy as before. **c** Shear strain variations, ε_{xy}, surrounding the rupture tip predicted by LEFM for $v = 0.96c_R$. The *blue square* denotes the strain gage rosette measurement location relative to the approaching rupture tip. Note the strong angular dependence that drives the violent oscillations in **b**. Adapted from Svetlizky and Fineberg (2014)

Rayleigh wave-speed, c_R, is presented. The surprisingly good agreement demonstrates that, at least in this material, the two conditions listed above are satisfied, and consequently the fields near the propagating rupture fronts are quantitatively described by the singular solutions predicted for shear (mode II) cracks in the framework of LEFM. It is interesting and important to note that the agreement to the LEFM singular fields was achieved with a velocity-independent fracture energy Γ, suggesting that the well-documented rate dependence of friction in PMMA (Baumberger and Caroli 2006) does not strongly influence the effective fracture energy.

The experiments described in Fig. 11 suggest that propagating sub-Rayleigh ruptures can be identified with mode II cracks. Let us now consider the question of rupture nucleation. This question is of great importance both in general and in the particular context of earthquake nucleation (see, for example, Ben-Zion and Sammis 2003; Ben-Zion and Rice 1997; Lapusta et al. 2000; Rubin and Ampuero 2005; Ampuero and Rubin 2008). If nucleation takes place as a Griffith-like process analogous to conventional crack initiation Lawn (1993), the nucleation length L_c—the critical size above which a slowly creeping patch becomes unstable—is determined by the physical conditions near the rupture tip and depends on the pre-stress level. Alternative friction-law dependent nucleation scenarios, however, are possible. For example, rate-and-state friction models (Ben-Zion 2001, 2008; Ben-Zion and Rice 1997; Lapusta et al. 2000; Rubin and Ampuero 2005; Ampuero and Rubin 2008) associate L_c with

a spatiotemporal friction instability of quasi-statically extending "creep patches" that is independent of the pre-stress level (Lapusta et al. 2000; Bar-Sinai et al. 2013). It is currently unclear which nucleation scenario, if any, is more physically realistic and, if so, under what conditions.

What is the origin and nature of the experimentally observed "slow fronts" (Rubinstein et al. 2004; Ben-David et al. 2010)? Recent theoretical work has suggested that they may be a direct result of the qualitative form of the friction law at the interface; the frictional constitutive law can also affect the existence and nature of propagating rupture fronts. To see this, consider a frictional interface separating two infinitely long elastic blocks of height H. When the interface is described by a conventional velocity-weakening friction law, e.g. a friction law in which the frictional resistance decreases from μ_s to μ_d with increasing slip velocity $\Delta\dot{u}$, steady-state propagating rupture front solutions can be found under some fixed shear displacement loading conditions. These solutions are analogous to those found for tensile cracks in a strip (Freund 1990), where the only difference is the role played by the residual stress σ_r. On the other hand, no steady-state solutions can be found under shear stress controlled conditions; as in the analogous Mode I problem of constant stress, frictional cracks should continually accelerate to c_R (as seen in Fig. 1).

What happens for a non-monotonic friction law? Such a friction law, where the steady-sliding frictional resistance is a non-monotonic function of the sliding velocity, with a maximum at very small velocities and a higher velocity minimum, is depicted in Fig. 12. This form is representative of a broad range of materials (Bar-Sinai et al. 2014). Consider again two infinitely long elastic blocks, now separated by an interface described by a steady sliding frictional resistance as in Fig. 12. A steady state propagating front is an object that smoothly connects two stable solutions in a homogeneous system, once the system is perturbed (e.g. via a stress gradient) and one of these solutions loses stability to the other. In the context of Fig. 12, stable solutions correspond to velocity-strengthening branches (i.e. when μ increases with increasing $\Delta\dot{u}$) and unstable (accelerating) solutions correspond to velocity-weakening branches (i.e. when μ decreases with increasing $\Delta\dot{u}$).

When the applied shear stress corresponds to the lower horizontal line in Fig. 12, below the minimum

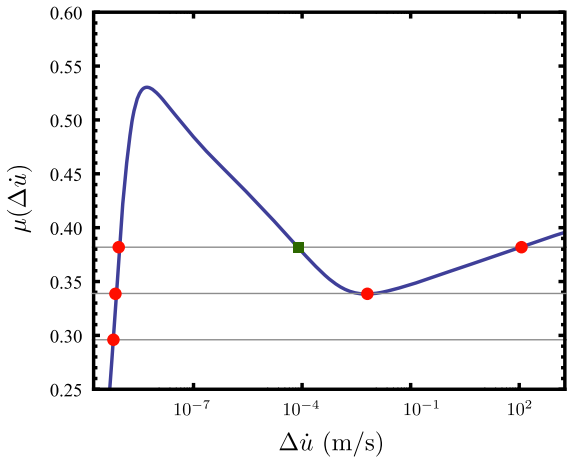

Fig. 12 A steady sliding friction curve $\mu(\Delta\dot{u})$, where $\Delta\dot{u}$ is the sliding velocity, which is typical of many materials (Bar-Sinai et al. 2014). The curve exhibits a non-monotonic behavior with a minimum after a small sliding velocity maximum. The *three horizontal lines* correspond to different levels of applied shear stress. A stable homogeneous solution is marked by a *red circle* and an unstable one by a *green square*

of the friction curve, there is only one stable homogeneous solution (marked by a red circle) and consequently no propagating front solutions exist. The situation is qualitatively different when the applied shear stress corresponds to the second horizontal line, which touches the friction curve at its minimum. In this case, there are two homogeneous solutions and a propagating front solution connecting the two is possible. Such a stably propagating solution was shown to exist (Bouchbinder et al. 2011; Bar-Sinai et al. 2012, 2013), where the characteristic slip velocity corresponds to the minimum of $\mu(\Delta\dot{u})$. The solution's propagation velocity could be significantly smaller than the elastic wave-speeds and independent of them (Bar-Sinai et al. 2012, 2013, 2015). Further increase of the applied shear stress (e.g. the upper horizontal line) produces a continuous spectrum of propagating front solutions with increasing propagation velocities, which eventually saturates at the relevant wave-speed (Bar-Sinai et al. 2012). At stresses above the minimum of the friction curve, an unstable homogeneous solution also exists (green square in Fig. 12).

Such propagating front solutions do not exist for friction laws that monotonically decrease with increasing slip velocity. This is an example in which the properties of the friction law have qualitative implications for the existence of steady state rupture fronts. Tran-

sient rupture fronts, which emerge in more complicated situations, may be considered to be short-lived excitations of these steady state propagating rupture fronts (Bouchbinder et al. 2011; Bar-Sinai et al. 2012, 2013). The existence of these solutions may therefore provide a possible explanation for slow interfacial rupture. The possible roles of non-monotonic friction laws in naturally occurring slow earthquakes have been recently explored (Weeks 1993; Shibazaki and Iio 2003; Kato 2003; Shibazaki and Shimamoto 2007; Hawthorne and Rubin 2013). While other mechanisms for the emergence of slow rupture have also been proposed, they generally involve invoking other physical ingredients such as higher dimensionality, spatial variation of the friction law and stress heterogeneities (Yoshida and Kato 2003; Liu and Rice 2005; Rubin 2008), dilation and pore pressure effects (Rubin 2008), and a discrete description of asperities, including stochasticity of various local quantities (Tromborg et al. 2014).

The frictional constitutive law can also give rise to crack-like objects which are not classical mode II cracks. For example, in the presence of viscous-friction (i.e. when the frictional resistance is linear in the sliding velocity, which may be relevant to both dry and lubricated frictional interfaces) the order of the displacement gradients singularity near the tip may differ from the common $\sqrt{r}$ singularity and depend on the friction law (Brener and Marchenko 2002; Brener et al. 2005). Furthermore, interesting physical properties such as a healing instability, a static threshold equivalent to the Griffith threshold and dissipation which is dominated by friction in a large interfacial region away from the tip region can emerge in certain situations (Brener and Marchenko 2002; Brener et al. 2005). Such frictional shear cracks were shown to be related to the experimentally observed self-healing slip pulses along an interface between a gelatin gel and a glass (Baumberger et al. 2002, 2003; Ronsin et al. 2011). These works established a clear connection between novel crack-like objects and frictional dynamics.

To this point we have described some recent insights obtained in the study of both sub-Rayleigh ($v < c_R$) and slow rupture fronts. We now briefly describe ruptures that propagate at velocities that are faster than c_R. These are commonly referred to as "super-shear" ruptures. Super-shear cracks have long been considered in the fracture literature (Freund 1990; Broberg 1999; Andrews 1976), but until they were observed in the beautiful experiments by Rosakis and coworkers (Rosakis et al. 1999), they were often considered to be of purely theoretical value. Since this first observation in weakly bonded homogeneous blocks that were ballistically loaded, mode II super-shear ruptures have been observed numerically (Gao et al. 2001; Liu et al. 2014; Shi et al. 2008) as well as in a variety of other scenarios that include frictional interfaces and quasi-static loading (Rubinstein et al. 2004; Ben-David et al. 2010; Xia et al. 2004; Passelegue et al. 2013).

These recent experiments have revealed that super-shear ruptures are not rare at all, but appear in many cases when the initial energy stored in the surrounding material is much higher than that needed to drive a running crack. When loaded ballistically, super-shear states are observed only for relatively high projectile velocities (Rosakis et al. 1999), whereas in frictional sliding super-shear ruptures are initiated when the initial shear stresses are very large [e.g. when the "friction coefficient" is significantly greater than $\mu_s \simeq 0.6$ in PMMA (Ben-David et al. 2010) or granite (Passelegue et al. 2013)]. In addition to laboratory experiments and simulations, there is growing evidence that super-shear propagation can occur in earthquakes (Bouchon and Vallee 2003; Bouchon et al. 2001; Dunham and Archuleta 2004; Vallee and Dunham 2012; Mello et al. 2014) which is often associated with extreme damage.

While their existence in no longer in doubt, a more precise characterization of super-shear ruptures is needed. It is not yet clear, for example, if the observed super-shear ruptures along frictional interfaces indeed correspond to "textbook" super-shear solutions of mode II fracture (in analogy to the characterization performed in Fig. 11 for sub-Rayleigh ruptures).

The nucleation of super-shear ruptures is an important and still open question. While a number of scenarios for the nucleation of such modes have been suggested (Xia et al. 2004; Broberg 1999; Andrews 1976; Dunham et al. 2003), it is not yet entirely clear how the transition from sub-Rayleigh to super-shear ruptures comes about. A common theme among these different scenarios is that sufficient elastic energy becomes available in close proximity to a frictional interface. This has been shown to take place either via the interaction of the crack front with localized perturbations (Dunham et al. 2003), via radiation from an existing sub-Rayleigh front (Xia et al. 2004; Broberg 1999; Andrews 1976; Madariaga 1977), or simply due to sufficient pre-

existing strain energy surrounding the interface prior to nucleation (Ben-David et al. 2010). This last scenario has been suggested as a necessary one for mode I super-shear cracks in rubber-like materials (Marder 2006; Chen et al. 2011; Buehler et al. 2003) and may well be relevant for mode II cracks as well.

7 Future directions

In the previous sections we highlighted a number of interesting topics in dynamic fracture that, in our opinion, have progressed significantly in recent years. Below we list a number of promising research directions that are related to each topic.

7.1 Equation of motion for a crack

The work reviewed in Sect. 2 has conclusively shown that the equation(s) of motion for simple cracks are correct, as long as a crack remains simple. The energy balance criterion works perfectly as long as the propagation direction of the crack is both prescribed and the relevant boundary conditions are properly accounted for. We do not have, as yet, a general equation for determining the path of dynamic cracks. One such equation was discussed in Sect. 4.3 and was applied to crack oscillations in 2D. Other interesting work has been performed in relation to dynamic path selection in crystalline materials (Marder 2004; Atrash and Sherman 2012). Nevertheless, there is still much more to be done in this direction. Recent post-mortem analysis of fracture surface markings in PMMA (Guerra et al. 2012) has suggested that microscopic crack front motion takes place via the merging of voids ahead of the crack tip, at velocities significantly below the mean crack front velocity. Whereas these observations are perfectly compatible with LEFM, they raise an interesting question of size effects; how large do inhomogeneities have to be in order to invalidate the continuum description of crack front propagation? Whereas the interaction of crack fronts with single asperities has been explored in the LEFM framework (Ramanathan and Fisher 1997; Morrissey and Rice 1998, 2000), it will be interesting to see how/if this framework generalizes to a large number/size of defects. Is there a scale where the crack front loses its identity as a coherent entity?

7.2 Nonlinear elasticity and soft solids

LEFM, as well as the weakly nonlinear theory, assume a "base" state of zero background strain. This approximation works well for most "standard" brittle materials, such as glass, brittle ceramics or brittle acrylics. Lately, new classes of materials are becoming available that join natural rubber as elastic, yet brittle, materials that can sustain large background strains prior to fracture. The fracture resistance of some of these synthetic materials, such as double-network hydrogels made of ionically and covalently cross-linked networks (Gong et al. 2003; Gong 2010; Sun et al. 2012; Rose et al. 2013, 2014; Li et al. 2014), can be made to be enormous and new applications are expected to abound (Lin et al. 2011; Rose et al. 2014). In addition to such "chemical gels", there is also clear experimental evidence that elastic nonlinearities are important to fracture processes in "physical gels" (Ronsin et al. 2014), i.e. weakly cross-linked elastomers, that are important in biological applications. As all of these materials exhibit large strains prior to fracture, existing theoretical frameworks should be extended to large background strains. Very recent experiments have shown these effects to be important and the first extension of weakly nonlinear fracture mechanics to moderate background strains has been developed (Goldman Boué et al. 2015b). This framework might also apply to the related topic of the strength of tough pressure-sensitive adhesives, such as adhesive tapes (Cortet et al. 2013; Dalbe et al. 2014a, b).

7.3 Instabilities in dynamic fracture

The recent advances reviewed here may provide us with some tools needed to initiate a more complete understanding of dynamic instabilities. From these results, it appears that to fully understand these phenomena, the framework of fracture mechanics should be extended to systematically include 3D crack propagation. The near vicinity of the crack tip (e.g. the process zone) is not simply a passive region that is needed to dissipate energy, but, as we saw in Sect. 4.3, the process zone can actively feed back to the elastic fields driving the crack to produce unstable behavior. The 3D form of micro-branches implies that these effects entail a finite-size perturbation to the crack front. Initial studies of crack front waves considered only

linear perturbations to an LEFM-described front. Further development of a nonlinear description of crack front behavior may provide a way to better explore crack front interactions with either active noise sources (e.g. micro-branches) or quenched noise, such as material inhomogeneities. Other promising directions to describe 3D effects include the use of phase-field models to provide an accessible way to couple the nonlinear elastic fields to dynamic models describing the crack tip. Some initial steps in this direction have been accomplished (Henry and Adda-Bedia 2013; Leblond et al. 2011; Pons and Karma 2010), but there are still a number of open questions about how to ensure the physical predictive power of these models.

7.4 Fracture-based descriptions of friction

Recent experiments have demonstrated that frictional motion is intimately related to dynamic fracture. A fundamental understanding of these important processes must, therefore, involve rapid fracture. While many related issues has been extensively discussed in the geophysical literature (Das 2003; Ben-Zion 2008), careful examination of frictional "fracture" in well-controlled laboratory experiments has only began to emerge. In Sect. 6, a few aspects of this research direction have been mentioned. Different modes of earthquake-like rupture states are expected to abound in these systems; these range from sustained slow fracture modes to super-shear rupture. The results described in Fig. 11, for example, relate to dry and rough frictional interfaces formed by *identical* materials. It would be interesting to make a similar comparison to analytical results that describe mode II super-shear cracks along homogeneous interfaces, whose singular properties are predicted to be quite different from those of standard cracks (Broberg 1999). Entirely different classes of rupture, that include "self-healing" pulse-like as well as crack-like rupture states, are believed be generated within *bimaterial* interfaces; interfaces formed by two materials having different elastic properties (Ben-Zion 2008; Weertman 1980; Ben-Zion and Andrews 1998; Cochard and Rice 2001; Gerde and Marder 2001; Perrin et al. 1995). Recent experimental results (Lykotrafitis et al. 2006; Lu et al. 2010) have demonstrated the existence of a number of these interesting modes. Crack-like modes may also be excited within lubricated interfaces (Brener and Marchenko 2002; Brener et al. 2005). Like super-shear states, these rupture modes are predicted to possess functional forms that are still singular, but with singularities that may be entirely different from the square root singularity generally associated with cracks.

In conclusion, in this perspectives piece we have presented a number of new and interesting developments in the field of dynamic fracture. The examples noted are all important, but are by no means all-inclusive. We have endeavored to show that dynamic fracture is not only important in itself, but is critical to our fundamental understanding of topics ranging from the strength of new "super-tough" materials to the dynamics of earthquakes. We expect that these developments will continue into the next decades.

Acknowledgments E. B. and J. F. acknowledge support from the James S. McDonnell Fund (Grant No. 220020221), E. B. acknowledges support from the Minerva Foundation with funding from the Federal German Ministry for Education and Research, the Harold Perlman Family Foundation and the William Z. and Eda Bess Novick Young Scientist Fund. J. F. acknowledges support from the European Research Council (Grant No. 267256), and the Israel Science Foundation (Grant 76/11).

References

Adda-Bedia M, Arias R, Ben-Amar M, Lund F (1999) Dynamic instability of brittle fracture. Phys Rev Lett 82(11):2314–2317

Adda-Bedia M (2005) Brittle fracture dynamics with arbitrary paths III. The branching instability under general loading. J Mech Phys Solids 53(1):227–248

Adda-Bedia M, Arias RE, Bouchbinder E, Katzav E (2013) Dynamic stability of crack fronts: out-of-plane corrugations. Phys Rev Lett 110(1):014302

Adda-Bedia M, Pomeau Y (1995) Crack instabilities in a heated glass strip. Phys Rev E 52:4105–4113

Ampuero JP, Rubin AM (2008) Earthquake nucleation on rate and state faults aging and slip laws. J Geophys Res 113(B1):B01302

Andrews DJ (1976) Rupture velocity of plane strain shear cracks. J Geophys Res Solid Earth 81:5679–5687

Aranson IS, Kalatsky VA, Vinokur VM (2000) Continuum field description of crack propagation. Phys Rev Lett 85(1):118–121

Atrash F, Sherman D (2012) Dynamic fracture instabilities in brittle crystals generated by thermal phonon emission: experiments and atomistic calculations. J Mech Phys Solids 60(5):844–856

Bar Sinai Y, Brener EA, Bouchbinder E (2012) Slow rupture of frictional interfaces. Geophys Res Lett 39:L03308

Bar-Sinai Y, Spatschek R, Brener EA, Bouchbinder E (2013) Instabilities at frictional interfaces: creep patches, nucleation, and rupture fronts. Phys Rev E 88(6):060403

Bar-Sinai Y, Spatschek R, Brener EA, Bouchbinder E (2014) On the velocity-strengthening behavior of dry friction. J Geophys Res Solid Earth 119(3):1738–1748

Bar-Sinai Y, Spatschek R, Brener EA, Bouchbinder E (2015) Velocity-strengthening friction significantly affects interfacial dynamics, strength and dissipation. Sci Rep 5:7841

Baumberger T, Caroli C, Ronsin O (2002) Self-healing slip pulses along a gel/glass interface. Phys Rev Lett 88:075509

Baumberger T, Caroli C, Ronsin O (2003) Self-healing slip pulses and the friction of gelatin gels. Eur Phys J E 11(1):85–93

Baumberger T, Caroli C, Martina D (2006) Solvent control of crack dynamics in a reversible hydrogel. Nat Mater 5(7):552–555

Baumberger T, Caroli C, Martina D, Ronsin O (2008) Magic angles and cross-hatching instability in hydrogel fracture. Phys Rev Lett 100:178303

Baumberger T, Caroli C (2006) Solid friction from stick-slip down to pinning and aging. Adv Phys 55(3–4):279–348

Baumberger T, Ronsin O (2010) A convective instability mechanism for quasistatic crack branching in a hydrogel. Eur Phys J E 31(1):51–58

Ben-David O, Cohen G, Fineberg J (2010) The dynamics of the onset of frictional slip. Science 330(6001):211–214

Ben-David O, Fineberg J (2011) Static friction coefficient is not a material constant. Phys Rev Lett 106(25):254301

Ben-Zion Y (2001) Dynamic ruptures in recent models of earthquake faults. J Mech Phys Solids 49(9):2209–2244

Ben-Zion Y (2008) Collective behavior of earthquakes and faults: continuum-discrete transitions, progressive evolutionary changes, and different dynamic regimes. Rev Geophys 46(4):RG4006

Ben-Zion Y, Andrews DJ (1998) Properties and implications of dynamic rupture along a material interface. Bull Seismol Soc Am 88:1085–1094

Ben-Zion Y, Rice JR (1997) Dynamic simulations of slip on a smooth fault in an elastic solid. J Geophys Res 102(B8):17771

Ben-Zion Y, Sammis CG (2003) Characterization of fault zones. Pure Appl Geophys 160(3–4):677–715

Bergkvist H (1974) Some experiments on crack motion and arrest in polymethylmethacrylate. Eng Fract Mech 6:621–626

Beroza GC, Ide S (2011) Slow earthquakes and nonvolcanic tremor. Annu Rev Earth Planet Sci 39:271–296

Bhat HS, Dmowska R, King GCP, Klinger Y, Rice JR (2007) Off-fault damage patterns due to supershear ruptures with application to the 2001 M-w 8.1 Kokoxili (Kunlun) Tibet earthquake. J Geophys Res Solid Earth 112(B6):B06301

Bonamy D, Bouchaud E (2011) Failure of heterogeneous materials: a dynamic phase transition? Phys Rep Rev Sect Phys Lett 498(1):1–44

Bonamy D, Ravi-Chandar K (2003) Interaction of shear waves and propagating cracks. Phys Rev Lett 91(23):235502

Bouchaud E, Bouchaud JP, Fisher DS, Ramanathan S, Rice JR (2002) Can crack front waves explain the roughness of cracks? J Mech Phys Solids 50(8):1703–1725

Bouchbinder E, Hentschel HGE, Procaccia I (2003) Dynamical instabilities of quasistatic crack propagation under thermal stress. Phys Rev E 68:036601

Bouchbinder E, Mathiesen J, Procaccia I (2005) Branching instabilities in rapid fracture: dynamics and geometry. Phys Rev E 71:056118

Bouchbinder E, Livne A, Fineberg J (2008) Weakly nonlinear theory of dynamic fracture. Phys Rev Lett 101(26):264302

Bouchbinder E, Livne A, Fineberg J (2009) The 1/r singularity in weakly nonlinear fracture mechanics. J Mech Phys Solids 57(9):1568–1577

Bouchbinder E (2009) Dynamic crack tip equation of motion: high-speed oscillatory instability. Phys Rev Lett 103(16):164301

Bouchbinder E (2010) Autonomy and singularity in dynamic fracture. Phys Rev E 82:015101

Bouchbinder E, Fineberg J, Marder M (2010a) Dynamics of simple cracks. Annu Rev Condens Matter Phys 1(1):371–395

Bouchbinder E, Livne A, Fineberg J (2010b) Weakly nonlinear fracture mechanics: experiments and theory. Int J Fract 162:3–20

Bouchbinder E, Brener EA, Barel I, Urbakh M (2011) Slow cracklike dynamics at the onset of frictional sliding. Phys Rev Lett 107(23):235501

Bouchbinder E, Goldman T, Fineberg J (2014) The dynamics of rapid fracture: instabilities, nonlinearities and length scales. Rep Prog Phys 77(4):046501

Bouchbinder E, Procaccia I (2007) Oscillatory instability in two-dimensional dynamic fracture. Phys Rev Lett 98:124302

Bouchon M, Bouin MP, Karabulut H, Toksoz MN, Dietrich M, Rosakis AJ (2001) How fast is rupture during an earthquake? New insights from the 1999 Turkey earthquakes. Geophys Res Lett 28(14):2723–2726

Bouchon M, Vallee M (2003) Observation of long supershear rupture during the magnitude 8.1 Kunlunshan earthquake. Science 301(5634):824–826

Boudet JF, Ciliberto S, Steinberg V (1995) Experimental study of the instability of crack propagation in brittle materials. Europhys Lett 30:337–342

Bowden FP, Tabor D (2001) The friction and lubrication of solids, 2nd edn. Oxford University Press, New York

Braun OM, Barel I, Urbakh M (2009) Dynamics of transition from static to kinetic friction. Phys Rev Lett 103(19):194301

Brener EA, Malinin SV, Marchenko VI (2005) Fracture and friction: stick-slip motion. Eur Phys J E 17(1):101–113

Brener EA, Marchenko VI (2002) Frictional shear cracks. JETP Lett 76(4):211–214

Broberg KB (1960) The propagation of a brittle crack. Arkiv fur Fysik 18:159–192

Broberg KB (1999) Cracks and fracture. Academic Press, San Diego

Buehler MJ, Abraham FF, Gao H (2003) Hyperelasticity governs dynamic fracture at a critical length scale. Nature 426:141–146

Buehler MJ, Gao H (2006) Dynamic fracture instabilities due to local hyperelasticity at crack tips. Nature 439:307–310

Burridge R, Conn G, Freund LB (1979) The stability of a rapid mode-II shear crack with finite cohesive traction. J Geophys Res 84(NB5):2210–2222

Capozza R, Urbakh M (2012) Static friction and the dynamics of interfacial rupture. Phys Rev B 86(8):085430

Chen CH, Zhang HP, Niemczura HPJ, Ravi-Chandar K, Marder M (2011) Scaling of crack propagation in rubber sheets. Europhys Lett 96:36009

Cochard A, Rice JR (2001) Fault rupture between dissimilar materials: Ill-posedness, regularization, and slip-pulse response. J Geophys Res B 105(11):25891–25907
Cooke ML, Pollard DD (1996) Fracture propagation paths under mixed mode loading within rectangular blocks of polymethyl methacrylate. J Geophys Res 101(B2):3387–3400
Corson F, Adda-Bedia M, Henry H, Katzav E (2009) Thermal fracture as a framework for quasi-static crack propagation. Int J Fract 158:1–14
Cortet PP, Dalbe MJ, Guerra C, Cohen C, Ciccotti M, Santucci S, Vanel L (2013) Intermittent stick-slip dynamics during the peeling of an adhesive tape from a roller. Phys Rev E 87(2):022601
Cotterell B, Rice JR (1980) Slightly curved or kinked cracks. Int J Fract 14:155
Cramer T, Wanner A, Gumbsch P (2000) Energy dissipation and path instabilities in dynamic fracture of silicon single crystals. Phys Rev Lett 85:788–791
Cross MC, Hohenberg PC (1993) Pattern-formation outside of equilibrium. Rev Mod Phys 65(3):851–1112
Dalbe MJ, Santucci S, Cortet PP, Vanel L (2014a) Strong dynamical effects during stick-slip adhesive peeling. Soft Matter 10(1):132–138
Dalbe MJ, Santucci S, Vanel L, Cortet PP (2014b) Peeling-angle dependence of the stick-slip instability during adhesive tape peeling. Soft Matter 10(48):9637–9643
Dally JW (1979) Dynamic photoelastic studies of fracture. Exp Mech 19(10):349–361
Das S (2003) Spontaneous complex earthquake rupture propagation. Pure Appl Geophys 160(3–4):579–602
Deegan RD, Petersan P, Marder M, Swinney HL (2002) Oscillating fracture paths in Rubber. Phys Rev Lett 88:14304
Dieterich J (1979) Modelling of rock friction: 1. Experimental results and constitutive equations. J Geophys Res Solid Earth 84:2161–2168
Dieterich JH, Kilgore BD (1996) Imaging surface contacts: power law contact distributions and contact stresses in quartz, calcite, glass and acrylic plastic. Tectonophysics 256(1–4):219–239
Dunham EM, Favreau P, Carlson JM (2003) A supershear transition mechanism for cracks. Science 299(5612):1557–1559
Dunham EM, Archuleta RJ (2004) Evidence for a supershear transient during the 2002 Denali fault earthquake. Bull Seismol Soc Am 94(6):S256–S268
Ebert U, van Saarloos W, Caroli C (1997) Propagation and structure of planar streamer fronts. Phys Rev E 55(2):1530–1549
Eshelby JD (1971) Fracture mechanics. Sci Prog 59:161–179
Falk ML, Needleman A, Rice JR (2001) A critical evaluation of cohesive zone models of dynamic fractur. J Phys IV 11(PR5):43–50
Fineberg J, Gross SP, Marder M, Swinney HL (1991) Instability in dynamic fracture. Phys Rev Lett 67(4):457–460
Fineberg J, Marder M (1999) Instability in dynamic fracture. Phys Rep 313:1–108
Fineberg J, Steinberg V (1987) Vortex-front propagation In Rayleigh–Benard convection. Phys Rev Lett 58(13):1332–1335
Fleck M, Pilipenko D, Spatschek R, Brener EA (2011) Brittle fracture in viscoelastic materials as a pattern-formation process. Phys Rev E 83(4):046213
Freund LB (1979) Mechanics of dynamic shear crack-propagation. J Geophys Res 84(NB5):2199–2209
Freund LB (1990) Dynamic fracture mechanics. Cambridge University Press, Cambridge
Gabriel AA, Ampuero JP, Dalguer LA, Mai PM (2013) Source properties of dynamic rupture pulses with off-fault plasticity. J Geophys Res Solid Earth 118(8):4117–4126
Gao H (1996) A theory of local limiting speed in dynamic fracture. J Mech Phys Solids 44:1453–1474
Gao H, Huang Y, Abraham FF (2001) Continuum and atomistic studies of intersonic crack propagation. J Mech Phys Solids 49:2113–2132
Gao H, Rice JR (1989) A first-order perturbation analysis of crack trapping by arrays of obstacles. J Appl Mech Trans ASME 56(4):828–836
Gerde E, Marder M (2001) Friction and fracture. Nature 413:285–288
Goldman Boué T, Cohen G, Fineberg J (2015a) Origin of the microbranching instability in rapid cracks. Phys Rev Lett 114:054301
Goldman Boué T, Harpaz R, Fineberg J, Bouchbinder E (2015b) Failing softly: a fracture theory of highly-deformable materials. Soft Matter 11(19):3812–3821
Goldman T, Livne A, Fineberg J (2010) Acquisition of inertia by a moving crack. Phys Rev Lett 114(11):114301
Goldman T, Harpaz R, Bouchbinder E, Fineberg J (2012) Intrinsic nonlinear scale governs oscillations in rapid fracture. Phys Rev Lett 108(10):104303
Gol'dstein RV, Salganik RL (1974) Brittle fracture of solids with arbitrary cracks. Int J Fract 10(4):507–523
Gong J, Katsuyama Y, Kurokawa T, Osada Y (2003) Double-network hydrogels with extremely high mechanical strength. Adv Mater 15(14):1155–1158
Gong JP (2010) Why are double network hydrogels so tough? Soft Matter 6(12):2583
Gross SP, Fineberg J, Marder M, McCormick W, Swinney HL (1993) Acoustic emissions from rapidly moving cracks. Phys Rev Lett 71(19):3162–3165
Guerra C, Scheibert J, Bonamy D, Dalmas D (2012) Understanding fast macroscale fracture from microcrack post mortem patterns. Proc Natl Acad Sci U S A 109(2):390–394
Guozden TM, Jagla EA, Marder M (2010) Supersonic cracks in lattice models. Int J Fract 162:107
Hakim V, Karma A (2005) Crack path prediction in anisotropic brittle materials. Phys Rev Lett 95(23):235501
Hakim V, Karma A (2009) Laws of crack motion and phase-field models of fracture. J Mech Phys Solids 57:342–368
Harpaz R, Bouchbinder E (2012) A nonlinear symmetry breaking effect in shear cracks. J Mech Phys Solids 60(10):1703–1709
Hawthorne JC, Rubin aM (2013) Laterally propagating slow slip events in a rate and state friction model with a velocity-weakening to velocity-strengthening transition. J Geophys Res Solid Earth 118(7):3785–3808
Heizler SI, Kessler DA, Levine H (2002) Mode I fracture in a nonlinear lattice with viscoelastic forces. Phys Rev E 66:016 126
Henry H (2008) Study of the branching instability using a phase field model of inplane crack propagation. Europhys Lett (EPL) 83(1):16004

Henry H, Adda-Bedia M (2013) Fractographic aspects of crack branching instability using a phase-field model. Phys Rev E 88(6):060401

Henry H, Levine H (2004) Dynamic instabilities of fracture under biaxial strain using a phase field model. Phys Rev Lett 93(10):105504

Hodgdon JA, Sethna JP (1993) Derivation of a general three-dimensional crack-propagation law: a generalization of the principle of local symmetry. Phys Rev B 47(9):4831–4840

Holland D, Marder M (1999) Cracks and atoms. Adv Mater 11:793–806

Holzapfel GA (2000) Nonlinear solid mechanics. Wiley, Chichester

Hui CL, Ruina A (1995) Why K? High order singularities and small scale yielding. IJF 72:97–120

Hull D (1997) Interpretation of river line steps associated with the growth of cracks. In: Chan KS (ed) Cleavage fracture: George R. Irwin symposium. The Metallurgical Society, Warrendale, pp 59–68

Irwin GR (1957) Analysis of stresses and strains near the end of a crack traversing a plate. J Appl Mech 24:361–364

Kammer DS, Yastrebov VA, Spijker P, Molinari JF (2012) On the propagation of slip fronts at frictional interfaces. Tribol Lett 48(1):27–32

Kammer DS, Radiguet M, Ampuero JP, Molinari JF (2015) Linear elastic fracture mechanics predicts the propagation distance of frictional slip. Tribol Lett 57:23

Karma A, Lobkovsky AE (2004) Unsteady crack motion and branching in a phase-field model of brittle fracture. Phys Rev Lett 92(24):245510

Katano Y, Nakano K, Otsuki M, Matsukawa H (2014) Novel friction law for the static friction force based on local precursor slipping. Sci Rep 4:6324

Kato N (2003) A possible model for large preseismic slip on a deeper extension of a seismic rupture plane. Earth Planet Sci Lett 216(1–2):17–25

Kessler DA, Levine H (2001) Nonlinear lattice model of viscoelastic mode III fracture. Phys Rev E 63:016118

Kessler DA, Levine H (2003) Does the continuum theory of dynamic fracture work? Phys Rev E 68(3):036118

Knauss WG (1970) An observation of crack propagation in anti-plane shear. Int J Fract Mech 6(2):183–187

Kobayashi AS, Mall S (1978) Dynamic fracture toughness of Homalite-100. Exp Mech 18(1):11–18

Kolvin I, Cohen G, Fineberg J (2015) Crack front dynamics: the interplay of singular geometry and crack instabilities. Phys Rev Lett 114(17):175501

Kostrov BV (1975) On the crack propagation with variable velocity. Int J Fract 11(1):47–56

Krug J, Spohn H (1991) Kinetic roughening of growing interfaces. Cambridge University Press, Cambridge

Langer JS, Lobkovsky AE (1998) Critical examination of cohesive-zone models in the theory of dynamic fracture. J Mech Phys Solids 46(9):1521–1556

Lapusta N, Rice JR, Ben-Zion Y, Zheng G (2000) Elastodynamic analysis for slow tectonic loading with spontaneous rupture episodes on faults with rate- and state-dependent friction. J Geophys Res 105(B10):23765

Latour S, Schubnel A, Nielsen S, Madariaga R, Vinciguerra S (2013) Characterization of nucleation during laboratory earthquakes. Geophys Res Lett 40(19):5064–5069

Lawn B (1993) Fracture in brittle solids, 2nd edn. Cambridge University Press, Cambridge

Lazarus V, Leblond JB, Mouchrif SE (2001) Crack front rotation and segmentation in mixed mode I plus III or I + II + III. Part II: comparison with experiments. J Mech Phys Solids 49(7):1421–1443

Lazarus V, Buchholz FG, Fulland M, Wiebesiek J (2008) Comparison of predictions by mode II or mode III criteria on crack front twisting in three or four point bending experiments. Int J Fract 153(2):141–151

Leblond JB, Karma A, Lazarus V (2011) Theoretical analysis of crack front instability in mode I + III. J Mech Phys Solids 59(9):1872–1887

Leblond JB, Lazarus V, Karma A (2015) Multiscale cohesive zone model for propagation of segmented crack fronts in mode I + III fracture. Int J Fract 191(1–2):167–189

Li J, Illeperuma WBK, Suo Z, Vlassak JJ (2014) Hybrid hydrogels with extremely high stiffness and toughness. ACS Macro Lett 3(6):520–523

Lin B, Mear ME, Ravi-Chandar K (2010) Criterion for initiation of cracks under mixed-mode I plus III loading. Int J Fract 165(2):175–188

Lin WC, Marcellan A, Hourdet D, Creton C (2011) Effect of polymer-particle interaction on the fracture toughness of silica filled hydrogels. Soft Matter 7(14):6578–6582

Liu C, Rosakis AJ, Freund LB (1993) The interpretation of optical caustics in the presence of dynamic non-uniform crack-tip motion histories: a study based on a higher order transient crack-tip expansion. Int J Solids Struct 30(7):875–897

Liu C, Bizzarri A, Das S (2014) Progression of spontaneous in-plane shear faults from sub-Rayleigh to compressional wave rupture speeds. J Geophys Res Solid Earth 119(11):8331–8345

Liu Y, Rice JR (2005) Aseismic slip transients emerge spontaneously in three-dimensional rate and state modeling of subduction earthquake sequences. J Geophys Res 110(B8):B08307

Livne A, Cohen G, Fineberg J (2005) Universality and hysteretic dynamics in rapid fracture. Phys Rev Lett 94(22):224301

Livne A, Ben-David O, Fineberg J (2007) Oscillations in rapid fracture. Phys Rev Lett 98(12):124301

Livne A, Bouchbinder E, Fineberg J (2008) The breakdown of linear elastic fracture mechanics near the tip of a rapid crack. Phys Rev Lett 101(26):264301

Livne A, Bouchbinder E, Svetlizky I, Fineberg J (2010) The near-tip fields of fast cracks. Science 327(5971):1359–1363

Lu X, Lapusta N, Rosakis AJ (2010) Pulse-like and crack-like dynamic shear ruptures on frictional interfaces: experimental evidence, numerical modeling, and implications. Int J Fract 163(1–2):27–39

Lykotrafitis G, Rosakis AJ, Ravichandran G (2006) Self-healing pulse-like shear ruptures in the laboratory. Science 313(5794):1765–1768

Madariaga R (1977) High-frequency radiation from crack (stress drop) models of earthquake faulting. Geophys J R Astron Soc 51(3):625–651

Maegawa S, Suzuki A, Nakano K (2010) Precursors of global slip in a longitudinal line contact under non-uniform normal loading. Tribol Lett 38(3):313–323

Marder M (1991) New dynamical equation for cracks. Phys Rev Lett 66(19):2484–2487

Marder M (2004) Cracks cleave crystals. Europhys Lett 66(3):364–370
Marder M (2006) Supersonic rupture of rubber. J Mech Phys Solids 54:491–532
Marder M, Gross S (1995) Origin of crack tip instabilities. J Mech Phys Solids 43:1–48
Marder M, Liu X (1993) Instability in lattice fracture. Phys Rev Lett 71:2417–2420
Marone C (1998) The effect of loading rate on static friction and the rate of fault healing during the earthquake cycle. Nature 391(6662):69–72
Mello M, Bhat HS, Rosakis AJ, Kanamori H (2014) Reproducing the supershear portion of the 2002 Denali earthquake rupture in laboratory. Earth Planet Sci Lett 387:89–96
Miller O, Freund LB, Needleman A (1999) Energy dissipation in dynamic fracture of brittle materials. Modell Simul Mater Sci Eng 7(4):573–586
Morrissey JW, Rice JR (1998) Crack front waves. J Mech Phys Solids 46(3):467–487
Morrissey JW, Rice JR (2000) Perturbative simulations of crack front waves. Crack front waves. J Mech Phys Solids 48(6–7):1229–1251
Movchan AB, Movchan NV, Willis JR (2005) Perturbation of a dynamic crack in an infinite strip. Mech Appl Math 58:333–347
Murnaghan F (1951) Finite deformation of an elastic solid. Wiley, New York
Obrezanova O, Movchan AB, Willis JR (2002) Dynamic stability of a propagating crack. J Mech Phys Solids 50(12):2637–2668
Palmer AC, Rice JR (1973) The growth of slip surfaces in the progressive failure of over-consolidated clay. Proc R Soc A Math Phys Eng Sci 332(1591):527–548
Passelegue FX, Schubnel A, Nielsen S, Bhat HS, Madariaga R (2013) From sub-Rayleigh to supershear ruptures during stick-slip experiments on crustal rocks. Science 340(6137):1208–1211
Perrin G, Rice JR, Zheng G (1995) Self-healing slip pulse on a frictional surface. J Mech Phys Solids 43(9):1461–1495
Pham VB, Bahr HA, Bahr U, Balke H, Weiss HJ (2008) Global bifurcation criterion for oscillatory crack path instability. Phys Rev E 77:066114
Pham KH, Ravi-Chandar K (2014) Further examination of the criterion for crack initiation under mixed-mode I plus III loading. Int J Fract 189(2):121–138
Pons AJ, Karma A (2010) Helical crack-front instability in mixed-mode fracture. Nature 464(7285):85–89
Radiguet M, Kammer DS, Gillet P, Molinari JF (2013) Survival of heterogeneous stress distributions created by precursory slip at frictional interfaces. Phys Rev Lett 111(16):164302
Ramanathan S, Fisher DS (1997) Dynamics and instabilities of planar tensile cracks in heterogeneous media. Phys Rev Lett 79(5):877–880
Rashetnia R, Mohammadi S (2015) Finite strain fracture analysis using the extended finite element method with new set of enrichment functions. Int J Numer Methods Eng 102:1316–1351
Ravi-Chandar K (1983) A note on the dynamic stress field near a propagating crack. Int J Solids Stuct 19(9):839–841
Ravi-Chandar K (2004) Dynamic fracture. Elsevier, Oxford
Ravi-Chandar K, Knauss WG (1984a) An experimental investigation into dynamic fracture: III. On steady-state crack propagation and crack branching. Int J Fract 26(1):141–154
Ravi-Chandar K, Knauss W (1984b) An experimental investigation into dynamic fracture: II. Microstructural aspects. Int J Fract 26(1):65–80
Ravi-Chandar K, Yang B (1997) On the role of microcracks in the dynamic fracture of brittle materials. J Mech Phys Solids 45:535–563
Rice JR (1968a) Fracture (chap. 3), vol 2. Academic Press, London, pp 191–311
Rice JR (1968b) A path independent integral and the approximate analysis of strain concentration by notches and cracks. J Appl Mech 35(2):379–386
Rice JR (1980) The mechanics of earthquake rupture. In: Dziewonski AM, Boschi E (eds) Physics of the Earth's interior. Italian Physical Society and North-Holland Publ. Co, Amsterdam, pp 555–649
Rice JR, Ruina AL (1983) Stability of steady frictional slipping. J Appl Mech 50:343–349
Robinson DP, Brough C, Das S (2006) The M-w 7.8, 2001 Kunlunshan earthquake: extreme rupture speed variability and effect of fault geometry. J Geophys Res Solid Earth 111:B08303
Ronsin O, Baumberger T, Hui CY (2011) Nucleation and propagation of quasi-static interfacial slip pulses. J Adhes 87(5):504–529
Ronsin O, Caroli C, Baumberger T (2014) Crack front echelon instability in mixed mode fracture of a strongly nonlinear elastic solid. EPL 105(3):34001
Rosakis AJ, Samudrala O, Coker D (1999) Cracks faster than the shear wave speed. Science 284(5418):1337–1340
Rosakis AJ, Freund LB (1981) The effect of crack tip plasticity on the determination of dynamic stress intensity factors by the optical method of caustics. J Appl Mech 48:302–308
Rose S, Marcellan A, Hourdet D, Creton C, Narita T (2013) Dynamics of hybrid polyacrylamide hydrogels containing silica nanoparticles studied by dynamic light scattering. Macromolecules 46(11):4567–4574
Rose S, Prevoteau A, Elziere P, Hourdet D, Marcellan A, Leibler L (2014) Nanoparticle solutions as adhesives for gels and biological tissues. Nature 505(7483):382–385
Rubin AM (2008) Episodic slow slip events and rate-and-state friction. J Geophys Res 113(B11):B11414
Rubin AM, Ampuero JP (2005) Earthquake nucleation on (aging) rate and state faults. J Geophys Res 110(B11):B11312
Rubinstein SM, Cohen G, Fineberg J (2004) Detachment fronts and the onset of dynamic friction. Nature 430(7003):1005–1009
Rubinstein SM, Barel I, Reches Z, Braun OM, Urbakh M, Fineberg J (2011) Slip sequences in laboratory experiments resulting from inhomogeneous shear as analogs of earthquakes associated with a fault edge. Pure Appl Geophys 168(12):2151–2166
Sagy A, Reches Z, Fineberg J (2002) Dynamic fracture by large extraterrestrial impacts as the origin of shatter cones. Nature 418(6895):310–313
Sagy A, Fineberg J, Reches Z (2004) Shatter cones: branched, rapid fractures formed by shock impact. J Geophys Res Solid Earth 109(B10):B10209

Sagy A, Cohen G, Reches Z, Fineberg J (2006) Dynamic fracture of granular material under quasi-static loading. J Geophys Res Solid Earth 111(B4):B003948
Scheibert J, Guerra C, Clari F, Dalmas D, Bonamy D (2010) Brittle–quasibrittle transition in dynamic fracture: an energetic signature. Phys Rev Lett 104(4):045501
Scholz C, Molnar P, Johnson T (1972) Detailed studies of frictional sliding of granite and implications for earthquake mechanism. J Geophys Res 77(32):6392
Scholz CH (1998) Earthquakes and friction laws. Nature 391(6662):37–42
Scholz C (2002) The mechanics of earthquakes and faulting, 2nd edn. Cambridge University Press, Cambridge
Sharon E, Gross S, Fineberg J (1995) Local crack branching as a mechanism for instability in dynamic fracture. Phys Rev Lett 74(25):5096–5099
Sharon E, Gross SP, Fineberg J (1996) Energy dissipation in dynamic fracture. Phys Rev Lett 76(12):2117–2120
Sharon E, Cohen G, Fineberg J (2001) Propagating solitary waves along a rapidly moving crack front. Nature 410(6824):68–71
Sharon E, Cohen G, Fineberg J (2002) Crack front waves and the dynamics of a rapidly moving crack. Phys Rev Lett 88(8):085503
Sharon E, Cohen G, Fineberg J (2004) Comment on "Interaction of shear waves and propagating cracks". Phys Rev Lett 93(9):099601
Sharon E, Fineberg J (1996) Microbranching instability and the dynamic fracture of brittle materials. Phys Rev B 54(10):7128–7139
Sharon E, Fineberg J (1998) Universal features of the microbranching instability in dynamic fracture. Philos Mag Part B 78(2):243–251
Sharon E, Fineberg J (1999) Confirming the continuum theory of dynamic brittle fracture for fast cracks. Nature 397(6717):333–335
Shi Z, Ben-Zion Y, Needleman A (2008) Properties of dynamic rupture and energy partition in a solid with a frictional interface. J Mech Phys Solids 56(1):5–24
Shibazaki B, Iio Y (2003) On the physical mechanism of silent slip events along the deeper part of the seismogenic zone. Geophys Res Lett 30(9):1489
Shibazaki B, Shimamoto T (2007) Modelling of short-interval silent slip events in deeper subduction interfaces considering the frictional properties at the unstable-stable transition regime. Geophys J Int 171(1):191–205
Sivashinsky GI (2002) Some developments in premixed combustion modeling. Proc Combust Inst 29:1737–1761
Slepyan LI (2002) Models and phenomena in fracture mechanics. Springer, Berlin
Smekal A (1953) Zum Bruchvogang bei sprodem Stoffrerhalten unter ein und mehrachsiegen Beanspringen. Osterr Ing Arch 7:49–70
Sommer E (1969) Formation of fracture 'lances' in glass. Eng Fract Mech 1:539–546
Spatschek R, Hartmann M, Brener E, Muller-Krumbhaar H, Kassner K (2006) Phase field modeling of fast crack propagation. Phys Rev Lett 96(1):015502
Spatschek R, Brener E, Karma A (2011) Phase field modeling of crack propagation. Philos Mag 91(1):75–95
Stephenson RA (1982) The equilibrium field near the tip of a crack for finite plane-strain of incompressible elastic-materials. J Elast 12:65–99
Sun JY, Zhao X, Illeperuma WRK, Chaudhuri O, Oh KH, Mooney DJ, Vlassak JJ, Suo Z (2012) Highly stretchable and tough hydrogels. Nature 489(7414):133–136
Svetlizky I, Fineberg J (2014) Classical shear cracks drive the onset of dry frictional motion. Nature 509(7499):205
Tanaka Y, Fukao K, Miyamoto Y, Sekimoto K (1998) Discontinuous crack fronts of three-dimensional fractures. Europhys Lett 43(6):664–670
Tromborg J, Scheibert J, Amundsen DS, Thogersen K, Malthe-Sorenssen A (2011) Transition from static to kinetic friction: insights from a 2D model. Phys Rev Lett 107(7):074301
Tromborg JK, Sveinsson HA, Scheibert J, Thogersen K, Amundsen DS, Malthe-Sorenssen A (2014) Slow slip and the transition from fast to slow fronts in the rupture of frictional interfaces. Proc Natl Acad Sci U S A 111(24):8764–8769
Vallee M, Dunham EM (2012) Observation of far-field Mach waves generated by the 2001 Kokoxili supershear earthquake. Geophys Res Lett 39:L05311
van Saarloos W (2003) Front propagation into unstable states. Phys Rep 386(2–6):29–222
Washabaugh PD, Knauss WG (1994) A reconciliation of dynamic crack velocity and Rayleigh wave speed in isotropic brittle solids. Int J Fract 65:97–114
Weeks JD (1993) Constitutive laws for high-velocity frictional sliding and their influence on stress drop during unstable slip. J Geophys Res 98(B10):17637
Weertman J (1980) Unstable slippage across a fault that separates elastic media of different elastic constants. J Geophys Res B 85:1455–1461
Williams ML (1957) On the stress distribution at the base of a stationary crack. J Appl Mech 24:109–114
Willis JR, Movchan NV, Movchan AB (2012) arXiv:1206.0870v1
Willis JR, Movchvan AB (1995) Dynamic weight functions for a moving crack. I. Mode I loading. J Mech Phys Solids 43:319–341
Willis JR, Movchan AB (1997) Three-dimensional dynamic perturbation of a propagating crack. J Mech Phys Solids 45(4):591–610
Xia KW, Rosakis AJ, Kanamori H (2004) Laboratory earthquakes: the sub-Rayleigh-to-supershear rupture transition. Science 303(5665):1859–1861
Xu G, Bower AF, Ortiz M (1994) An analysis of nonplanar crack-growth under mixed-mode loading. Int J Solids Struct 31(16):2167–2193
Yang B, Ravi-Chandar K (1996) On the role of the process zone in dynamic fracture. J Mech Phys Solids 44:1955–1976
Yoshida S, Kato N (2003) Episodic aseismic slip in a two-degree-of-freedom block-spring model. Geophys Res Lett 30(13):12–15